DEPARTMENT OF INTERNATIONAL AND EUROPEAN ECONOMIC STUDIES

ATHENS UNIVERSITY OF ECONOMICS AND BUSINESS

Climate Change, Natural World Preservation and the Emergence and Containment of Infectious Diseases

William Brock

Anastasios Xepapadeas

Working Paper Series

22-32

December 2022

Climate Change, Natural World Preservation and the Emergence and Containment of Infectious Diseases*

William Brock[1] and Anastasios Xepapadeas[2]

December 6, 2022

[1]University of Wisconsin at Madison and University of Missouri at Columbia. E-mail: wbrock@ssc.wisc.edu

[2]Department of Economics, University of Bologna and Athens University of Economics and Business. E-mail: anastasio.xepapadeas@unibo.it

Abstract

Scientific evidence suggests that anthropogenic impacts on the environment such as land use changes and climate change promote the emergence of infectious diseases in humans. We develop a two-region epidemic-economic model which unifies short-run disease containment policies with long-run policies which could control the drivers and the severity of infectious diseases. We structure our paper by linking a susceptible-infected-susceptible model with an economic model which includes land use choices for agriculture and climate change and accumulation of knowledge that supports land augmenting technical change. The contact number depends on short-run containment policies (e.g., lockdown, vaccination), and long-run policies affecting land use, the natural world and climate change. Climate change and land use changes have an additional cost in terms of infectious disease since

*The authors are grateful for valuable comments and suggestions from Spyros Tsangaris, and from the participants of the 10th SURED Conference, ETH Zurich, June 2022, the 27th EAERE Conference, University of Bologna, June 2022, and the 22nd ICABR Conference, University of Bologna, July 2022, at which earlier versions of this paper were presented.

they might increase the contact number in the long run. We derive optimal short-run containment controls for a Nash equilibrium between regions, and long-run controls for climate policy, land use and knowledge at an open loop Nash equilibrium and the social optimum and unify the short- and long-run controls. We explore the impact of ambiguity aversion and model misspecification in the unified model and provide simulations which support the theoretical model.

JELClassification: I18, Q54, D81

Keywords: infectious diseases, SIS model, natural world, climate change, land use, containment, Nash equilibrium, OLNE, social optimum, land augmenting technical change

1 Introduction

The COVID-19 crisis which emerged as both a serious human health emergency and a severe economic and social threat brought to the forefront the link between the anthropogenic impact on the natural world and the emergence of infectious diseases (IDs). This link has been recognized in the literature related to IDs but not as much in the economic literature prior to the advent of COVID-19. In the convergence model (Institute of Medicine 2008) for example, social, political and economic factors, along with environmental and genetic one, are leading factors in the emergence of IDs.

In exploring the mechanisms underlying the emergence of IDs and seeking a basis for the design of efficient prevention policy, the anthropogenic impact has been identified as an important factor by a number of researchers. Scientific evidence suggests that the total number and diversity of outbreaks and richness of IDs have increased significantly since 1980 (e.g., Smith et al. 2014). Jane Goodall (2020, p. 1):

> "...blamed the emergence of Covid-19 on the over-exploitation of the natural world, which has seen forests cut down, species made extinct and natural habitats destroyed. The coronavirus is thought to have made the jump from animals to humans late last year, possibly originating in a meat market in Wuhan, China. Intensive farming was also creating a reservoir of animal diseases that would spill over and hurt human society ... ."

ENSIA (2020), in a recent report, attributes the emergence of IDs such as COVID-19 to the destruction of habitats and loss of biodiversity, while Evans et al. (2020, p. 1) points out that:

> "ecological degradation increases the overall risk of zoonotic disease outbreaks originating from wildlife. The key "ingredients" that accentuate the risk of an emerging ID spillover event are activities (e.g., land conversion, creation of new habitat edges, wildlife trade and consumption, agricultural intensification) in or linked to areas of high biodiversity that elevate contact rates between humans and certain wildlife species."

Almada et al. (2017) stress the need to recognize that the relationship between humanity and natural systems is becoming an urgent global health priority. Watts et al. (2021), in the 2020 report of the Lancet countdown on health and climate change, emphasize that the changing climatic conditions are increasingly suitable for the transmission of numerous IDs, while the recent statement of the Lancet COVID-19 Commission (Lancet 2021, p. 21) indicates that:

> "...most known emerging diseases have originated in non-human animals, usually wildlife, and have emerged due to environmental and socioeconomic changes, such as land use change, agricultural expansion, and the wildlife trade."

In a more general context, Foley et al. (2005, p. 1 and Figure 3) point out that:

> "Global croplands, pastures, plantations, and urban areas have expanded in recent decades, accompanied by large increases in energy, water, and fertilizer consumption, along with considerable losses of biodiversity. Such changes in land use have enabled humans to appropriate an increasing share of the planet's resources, but they also potentially undermine the capacity of ecosystems to sustain food production, maintain freshwater and forest resources, regulate climate and air quality, and ameliorate infectious diseases."

A recent report on COVID-19 (The Independent Panel for Pandemic Preparedness and Response 2021, p. 19) stresses that:

> "Most of the new pathogens are zoonotic in origin. Driving their increasing emergence are land use and food production practices and population pressure. ... Accelerating tropical deforestation and incursion destroys wildlife health and habitat and speeds interchange between humans, wildlife and domestic animals. The threats to human, animal and environmental health are inextricably linked, and instruments to address them need to include climate change agreements and "30x30" global biodiversity targets."

Marani et al. (2021), using recent estimates of the rate of increase in disease emergence from zoonotic reservoirs associated with environmental change, suggest that the yearly probability of occurrence of extreme epidemics may increase due to deterioration of the natural world.

In the context of associating anthropogenic activities with the emergence of IDs, the contribution of climate change is also significant. Scientific evidence (e.g., Wyns 2020) suggests that infections which are transmitted through water or food, or by vectors such as mosquitoes and ticks, are highly sensitive to weather and climate conditions. The warmer, wetter and more variable conditions resulting from climate change are therefore making it easier to transmit diseases such as malaria, dengue fever, chikungunya, yellow fever, Zika virus, West Nile virus and Lyme disease in many parts of the world. Furthermore, permafrost thaw, caused by climate change, also carries consequences in terms of increased risks of ID outbreaks as a result of live pathogens liberated from thawed permafrost (Walsh et al. 2018, Meredith et al. 2019).

Nova et al. (2022, section 5) state that:

> "The activities that lead to anthropogenic disturbances of the environment – primarily, climate change, land-use change, urbanization, and global movement of humans, other organisms, and goods – affect societies and ecosystems in ways that favor the emergence of novel infectious diseases in human populations, expansions or shifts of diseases to new geographic regions, or re-emergence of diseases in various places"

and provide links between disease transmission and changes in temperature and rainfall as well as between changes in land use and disease incidence. For example, intensification of agriculture and industrial agriculture promotes *Aedes*-born viruses (e.g., dengue, Zika and yellow fever), Lyme disease and the Hendra virus.

Mora et al. (2022) provide evidence of a large number of pathogenic diseases and transmission pathways aggravated by climatic hazards, thus revealing the magnitude of the human health threat posed by climate change and the urgent need for aggressive actions to mitigate greenhouse gas (GHG) emissions. More specifically it was demonstrated in this review that 277 human pathogenic diseases can be aggravated by the broad array of climatic hazards triggered by ongoing emission of GHGs and include 58% of all infectious diseases known to have impacted humanity in recorded history. Furthermore, over 1,000 different pathways were identified in which the array of climatic hazards, via different transmission types, resulted in disease outbreaks by a taxonomic diversity of pathogens.

The discussion regarding the emergence of IDs suggests that the disease reservoirs, or ID hot spots, are located mainly in the tropical-subtropical climate zones in the Koepen-Geiger classification system (with the notable exception of permafrost). These climate zones contain hot spots for the natural world in terms of natural habitats, tropical forests and biodiversity. A disease outbreak which might emerge from the anthropogenic pressure on the disease reservoirs and the impact of climate change in these zones, if it occurs, diffuses to the rest of the world through regular transportation channels.

This discussion also suggests that the management of IDs can be analyzed in two time horizons. These are the short run, in which the ID has emerged and so containments policies such as lockdowns or vaccinations are in order, and the long run, in which policies focus on factors that affect the emergence and the severity of IDs, such as climate change and changes in land use.

In the present paper we set up a structure that incorporates the points made above about spatial and time separation. Thus, we develop a two-region model in which the tropical-subtropical zones are identified as region 1 and the temperate-snow zones as region 2. Sachs (2001) points out that agricultural technologies and health conditions are weak in the tropical relative to temperate zone, inducing a development gap. Thus a distinction between the two regions is relevant when land use and disease impacts are concerned.

To account for the time separation we consider two stages of analysis. In the first stage, which we call the short run, the outbreak of the ID has occurred. After the outbreak, both regions introduce policies to contain/eliminate the epidemic. Throughout the paper we assume that containment policies in the short run are decided in each region in a noncooperative way. This assumption draws on the fact that national health policies during the COVID period are decided by an independent national health system based on the specific characteristics of each country and not by a supranational authority. In designing containment policies in the short run, the regions do not consider any anthropogenic impacts (encroachment in the natural world or climate change) on the specific characteristics of the ongoing ID.

In the second stage, which we call the long run, the regions take into account the evolution of climate change and the encroachment on the natural world by agricultural activities on the specific characteristics related to the transmission of the ID. Changes in land use and encroachment in the natural world are induced mainly by industrial agriculture and by, for example, the need to satisfy the demand in wet markets, or the clearing of tropical forests to satisfy demands for products such as palm oil, meat or soybeans, or the establishment of industrial concentrated animal feeding operations. The long-run policies relate, therefore, to the regulation of land use which directly affects disease reservoirs, as well as to the adequate control of temperature increase relative to the preindustrial period through climate policy. An additional long-run policy explored is innovation as "land augmenting technical change" to show that costly innovation could help preserve the natural world and act as a prevention policy. In the long run we assume that the regions commit to decisions about land-use and climate policy that maximize own welfare, but we also characterize socially optimal solutions.[1]

The economic aspect of the recent pandemic has been analyzed mainly in terms of ways of controlling the pandemic – lockdowns, social distancing, vaccine development – and the associated benefits and costs of these policies (see, for example, Eichenbaum et al. 2020, Thunström et al. 2020, Berger

[1]Note that in the implementation of the Paris Accord, countries commit to carbon emissions paths. It is reasonable to assume that these paths are decided with reference to own welfare.

et al. 2021). The arguments put forward above make clear that in order to have efficient management of an emerging ID in both the short and the long run, there is a need for the development of coupled models of the economy and the natural world which include links associated with the ID reservoirs. This approach parallels the development of coupled models of the economy and climate through the appropriate integrated assessment models (IAMs). Augeraud-Véron et al. (2020) develop such a model in which the reduction of biodiversity *increases* the probability of emergence of zoonotic IDs. Boppart et al. (2020) propose "epidemic-economic (epi-econ) IAMs" and discuss economic instruments for controlling the epidemic after its emergence.

The contribution of our paper is the development of an epi-econ IAM that unifies disease containment policies which are appropriate when a disease has already occurred, with long-run policies which could control the drivers and the severity of IDs, land use and climate change, and agricultural innovation in our case. We structure our paper by linking a susceptible-infected-susceptible (SIS) model (e.g., Hethcote 1989, 2000) with an economic model which includes land-use choices for agriculture, climate change and land augmenting innovation.

In the SIS model, the contact number – which is the average number of adequate contacts with susceptibles of an infective during the infectious period – is not a fixed number as is standard in epidemiological models, but rather depends on policy parameters. In the short run there are containment policies (e.g., lockdown, social distancing, vaccination), while the long-run policies affect land use and the preservation of the natural world, and climate change. For the economy part, utility in each region is determined by a composite consumption good produced by labor, land devoted to agriculture, and energy. Climate change induced by energy use not only harms the composite consumption good but has an additional cost in terms of IDs since it might increase the contact number in the long run. Reduction of the natural world through changes in land use to expand agriculture also has a disease-cost in terms of the long-run contact number.

Given the high uncertainty associated with the structure and the parametrization of such a model, we provide a deterministic solution as a benchmark and compare it with outcomes derived under ambiguity associated with important parameters of the epi-econ model and ambiguity aversion.

Simulations of the model in both the short and the long run support our theoretical results.

2 An SIS model with containment

We follow Hethcote (1989) in considering a simple two-region SIS model, with regions indexed by $i = 1, 2$ for the tropical and temperate zones respectively. In the SIS model, infection does not confer immunity and individuals return to the susceptible class when they recover from infection. Since naturally-occurring births or deaths do not affect the behavior of the solution, we exclude them from the model for the sake of simplicity. Let susceptibles be denoted by S and the infective by I. Then the simple SIS model in terms of fractions of the total population can be written, in continuous time, as:

$$\dot{S}_i(t) = -\lambda_i(t) I_i(t) S_i(t) + \gamma_i I(t) \ , \ S(0) > 0 \tag{1}$$

$$\dot{I}_i(t) = \lambda_i(t) I_i(t) S_i(t) - \gamma_i I_i(t) \ , \ I_i(0) > 0 \tag{2}$$

$$I_i(t) + S_i(t) = 1 \ , \ i = 1, 2, \tag{3}$$

where $\lambda_i(t)$ is the regional contact rate, γ_i is the recovery or removal rate, and $z\sigma_i(t) = \lambda_i(t)/\gamma_i$ is the regional contact number. From (3), the dynamic system can be written as:

$$\begin{aligned} \dot{I}_i(t) &= \lambda_i(t) I_i(t) [1 - I_i(t)] - \gamma_i I_i(t) = \gamma_i I_i(t) \left[\frac{\lambda_i(t)(1 - I_i(t))}{\gamma_i} - 1 \right] \\ \dot{I}_i(t) &= \gamma_i I(t) [\sigma_i(t)(1 - I_i(t)) - 1] . \end{aligned} \tag{4}$$

From Hethcote (1989, theorem 4.1) we know that the solution for $S_i(t)$ approaches $1/\sigma_i(t)$ as $t \to \infty$ if $\sigma_i > 1$ and approaches 1 as $t \to \infty$ if $\sigma_i \leq 1$. In the context of an infinite-time planning horizon, the containment policy for an emerging ID takes place within a relatively small period of time. This implies that the SIS dynamics can be regarded as operating in fast time and the SIS system relaxes to the steady state $S = \min\{1, 1/\sigma\}$ and $I = 1 - S$ for any point in time. The contact number $\sigma_i(t)$ is the threshold quantity with the critical threshold value 1. We consider a time dependent contact number $\sigma_i(t)$ since it could refer to different emerging IDs at different points in time, or change over time in response to policies.

It is natural to assume that short-run containment and long-run prevention policies will target the contact number σ. The containment policies adopted for the COVID-19 pandemic included policies such as lockdowns, social distancing, quarantine and vaccination. In further specifying the contact number, we assume that costly containment such as vaccination will reduce the contact number, and that the output-producing labor force includes workers who are asymptomatic in the sense that, although infected, they do not have symptoms that require treatment, so they are neither in the infected class nor in quarantine but they can spread the disease and increase the contact number. The fraction of susceptible individuals should be increasing both in short-run containment policies once the disease emerges, but also in long-term prevention policies.

2.1 Coupling the epidemic model with the economy

Let $R(t)$ represent the natural world. In the sense of Goodall (2020), the natural world provides ecosystem services but also includes the viral-host reservoir for IDs. Human encroachment and destruction of the natural world emerges through changes in land use due mainly to land-intensive agriculture.[2] This introduces a trade-off between output production and ID emergence. Land-intensive industrial agriculture will reduce the natural world and facilitate the emergence of IDs. Let the natural world R_i in each region $i = 1, 2$ be defined as:

$$R_i(t) = \bar{L}_i(t) - L_{A,i}(t) \ , R_i(t) \geq 0, \tag{5}$$

where $\bar{L}_i(t)$ represents aggregate land availability, and $L_{A,i}(t)$ land devoted to agriculture in each region respectively. Reduction of R, as agricultural activities expand, indicates a reduction in the "distance" between human activities and disease reservoirs.[3]

In considering the impact of climate change, we assume that energy production by fossil fuels generates emissions of GHGs. Let $X(t)$ denote the stock of GHGs at time t relative to the preindustrial period with temporal

[2]We do not consider urbanization as another source of encroaching in the natural world.

[3]Restoration activities, such as reforestation, REDD+ policies and payments for ecosystem services, could increase R. In order to simplify the model, we do not include such activities.

evolution according to:

$$\dot{X}(t) = E_1(t) + E_2(t) - dX(t) \ , X(0) = X_{preindustrial}, \tag{6}$$

where $E_i(t)$ denotes emissions of GHGs from each region and d is a small GHG depreciation parameter. The accumulation of GHGs increases global average temperature relative to the preindustrial level (the temperature anomaly).[4] Using Matthews et al.'s (2009) approximation with Λ_i representing the regional transient climate response to cumulative carbon emissions (RTCRE)(see Leduc et al. 2016), the temperature anomaly in each region can be defined as

$$T_i(t) = \Lambda_i X(t) \,. \tag{7}$$

To incorporate the impacts of disease reservoirs and climate change in the evolution of the ID, we assume that once the disease emerges, the speed of the evolution of the infection could be variable, so we write (4) as:

$$\epsilon \dot{S}_i(t) = (1 - S_i(t)) \left[\lambda_i(t) S_i(t) - \gamma_i\right],$$

where ϵ is a small positive parameter. To provide a clear picture of a short-run containment policy, when both the land allocation and the regional temperatures are for all practical purposes fixed, we assume that $\epsilon \to 0$ so that when the infection emerges it relaxes fast to a steady state in which the fraction of susceptibles is determined as:

$$S_i(t) = \min\{1, 1/\sigma_i(t)\}, \frac{1}{\sigma_i(t)} = \tag{8}$$

$$\phi_{0i}(R_1(t), T_1(t)) + \phi_{1i}\left[b_i v(t) - m_i^{as} S_i(t) - q_j(1 - S_{jt})\right]$$

$$I_i(t) = 1 - \frac{1}{\sigma_i(t)} \ , \ i, j = 1, 2, \ i \neq j. \tag{9}$$

To simplify the mathematical exposition, when we write the optimality conditions we assume solutions in the zone $\sigma > 1$, or equivalently $S < 1$. In (8), ϕ_{0i} is the part of the contact rate $\lambda_i(t)$, or the fraction of susceptibles in the population $S_i(t)$, which is exogenous relative to short-run containment

[4]The accumulation equation (6) can be augmented by allowing for an increase of the natural world to slow down GHG accumulation in its capacity as a carbon sink. In this case agricultural expansion would further increase GHG accumulation and induce another positive feedback on the ID's contact number. This feedback could be an interesting area for further research.

policies. Since region 1 – the tropical/subtropical region – is regarded as containing the disease reservoirs, that is, the hot spot for the emergence of IDs, it is assumed that the value of ϕ_{0i} is determined by the current state of the natural world, $R_1(t)$, along with the current temperature anomaly, $T_1(t)$, in the region. In the long run, encroachment of the natural environment due to changes in land use and agricultural expansion – which "reduces" the natural world – along with global warming increase the contact number. We assume, therefore,

$$\phi_{0i}\left(R_1(t), T_1(t)\right) = \phi_{0iR}(R_1(t)) + \phi_{0iT}(T_1(t)) \geq 0, \tag{10}$$

where $\phi_{0iR}(R_1(t)), \phi_{0iT}(T_1(t))$ are concave increasing, convex decreasing respectively.

It should be noticed, however, that although in this paper we treat the tropics as the main source of emergent IDs, the concentrated animal feeding operations (CAFO) of the industrial agriculture in the temperate zones are also breeding grounds for IDs. If the expansion rate of IDs from CAFO proceeded at a rate comparable to the expansion rate of IDs from encroachment into the tropics (e.g., the deforestation rate of the Amazon for soybeans and cattle), then $R_2(t)$, and potentially $T_2(t)$ should affect ϕ_{0i}. Furthermore, Mora et al. (2022) list 1,006 different pathways for infectious diseases and around half of them are aggravated by climate change. Increasing temperatures might increase IDs coming out of temperate zone CAFOs, with animals being weakened by crowding and temperature stress, along with an increase in IDs coming out of the tropics. In trying to keep the theoretical model as tractable as possible, we do not take into account the impact of temperate zones and consider only the tropics as a source of IDs.[5] The function is decreasing in R_1 since it is assumed that augmenting the natural world in the South (i.e., reducing the relative size of the disease reservoirs and increasing their distance from human activities) reduces the contact number in both

[5]Although the relevant part of the contact rate in both regions depends on (R_1, T_1), the value of the contact rate need not be the same since it might depend on regional characteristics. That is, in general we may expect $\phi_{01}(\cdot,\cdot) \neq \phi_{02}(\cdot,\cdot)$. At this stage we were not able to provide a quantitative indication of this distinction. In the simulation part of the paper we make this distinction arbitrary since our objective is to validate the theoretical model. Undoubtedly issues related to the exact source of ID and the regional impacts of encroachments, CAFO, and increasing temperatures on the strength of emerging IDs is an an important area of future interdisciplinary research which will help to improve epi-econ models.

regions for any specific epidemic. On the other hand, global warming in the South increases the contact number for both regions, thus the function is increasing in T_1.

The term ϕ_{1i} characterizes the effectiveness of the containment policy in each region. In the short run, containment effort $v_i(t)$ reduces the contact number $\lambda_i(t)$, with effectiveness b_i and convex costs $c_i(v_i(t))$. The contact number increases by the potential spread of the disease by asymptomatic susceptible workers at the rate $m_i^{as} \geq 0$. We assume no migration between regions,[6] but individuals from one region can make short visits to the other by regular means of transportation (e.g., airplanes, ships). Infected individuals from region j traveling to region i infect individuals in region i proportionally to those infected in region j and vice versa, with proportionalities (q_j, q_i) respectively.

To link the economy with the epidemic model, we introduce a composite good:

$$Z_i(t) = C_i(t)^{\hat{a}_i} R_i(t)^{\hat{b}_i}, \hat{a}_i > 0, \hat{b}_i > 0, \hat{a}_i + \hat{b}_i < 1, i = 1, 2, \tag{11}$$

where C denotes material inputs in the composite good and R is "Nature's" input into the composite good, that is, ecosystem and biodiversity services. We define utility in each region as:[7]

$$U_i(Z_i(t)) = \ln\left(C_i(t)^{\hat{a}_i} R_i(t)^{\hat{b}_i}\right). \tag{12}$$

Material inputs are produced by labor, energy and land devoted to land-intensive industrial agriculture.[8] Labor is offered by susceptible individuals – who are not contained because of lockdowns – and is allocated among the non-agricultural part of the material inputs, $l_{c,i}$, and the land-intensive agriculture, $L_{A,i}$, devoted to agriculture can be augmented by innovation in agricultural technologies such as biotechnology. The accumulated stock

[6]Considering the possibility of infections from large scale migration flows between the two regions is beyond the scope of this paper, but it is an interesting area for further research.

[7]The log-linear utility function defined here can be regarded as a special case of a more general CES utility function of the form $Z = [aC^\tau + (1-a)R^\tau]^{1/\tau}$ with elasticity of substitution between material inputs and Nature $\sigma_e = 1/(1-\tau)$. This more general formulation might be used to explore the impact of complementarities between material inputs and Nature as measured by the inverse of the elasticity of substitution for $\sigma_e < 1$.

[8]To simplify the model, we do not include capital formation.

of knowledge, denoted by N, acts as Harrod augmenting technical change in the agricultural sector with innovation augmented land, or effective land input, defined as $(NL_{A,i})$.[9] Knowledge accumulates according to

$$\dot{N}(t) = n_2(t) - mN(t), \; N(0) = 1, \tag{13}$$

where $n_2(t)$ is the innovation flow undertaken by the developed North region 2 (e.g., R&D in bioengineering). The initial condition corresponds to the no innovation case, and m is a rate at which accumulated knowledge becomes obsolete. Innovation is costly and innovation costs c_{ni} fractionally lowers the composite good. It is assumed that knowledge has public good characteristics and, once accumulated in the North, it is freely available to both regions.[10]

Furthermore, costs related to labor use, $w_{l,h,i}$; land use, $c_{L,i}$; energy, $c_{h,E,i}$; containment of the epidemic, $c_{v,i}$; climate damages, ω_i; and R&D innovation in agriculture, $c_{n,2}$, fractionally lower the material part of the composite good.[11] After dropping t to ease notation, the composite good can be defined, for $i = 1, 2$, as:

$$\begin{aligned} C_i = {} & \left[\left(l_{c,i}^{\beta_{l,c,i}} E_{c,i}^{\beta_{c,E,i}}\right)^{\alpha_{c,i}}\right] \times \left[\left(l_{A,i}^{\beta_{l,A,i}} \left(NL_{A,i}\right)^{\beta_{L,A,i}} E_{A,i}^{\beta_{E,A,i}}\right)^{\alpha_{A,i}}\right] \times \\ & \exp\left[-\left(\sum_h w_{l,h,i} l_{h,i}\right) + \left(-c_{L,i} L_{A,i}\right) + \left(-\sum_h c_{E,h,i} E_{h,i}\right) + \right. \\ & \left. \left(\frac{-c_{v,i} v_i^2}{2}\right) + \left(\frac{-\omega_i T_i^2}{2}\right) + \left(\frac{-c_{n,i} n_2^2}{2}\right)\right] \end{aligned} \tag{14}$$

$$h = c, A, \; c_{n,1} = 0, c_{n,2} > 0 \tag{15}$$

$$S_i = l_{c,i} + l_{A,i} \tag{16}$$

$$R_i = \bar{L}_i - L_{A,i}. \tag{17}$$

[9] Barrows et al. (2014) point out that genetically engineering seed adoption can produce non-trivial savings of land from conversion to traditional agriculture as well as of emissions of GHGs. Agricultural productivity could be also improved by automation and robotics (e.g. Biswas and Aslekar 2022).

[10] An alternative assumption could be that knowledge is accumulated in both regions since many research labs in agriculture also do R&D for agricultural efficiency in tropical zones. In this case $n_2(t)$ in (13) should be replaced by $(n_1(t) + n_2(t))$. Another assumption could be that knowledge is a private good to each sector with partial diffusion across regions.

[11] REDD+ activities can be introduced by adding a term $RD0$ for REDD+ to the right hand side of (17) below and including a cost for these activities which fractionally reduces the composite good.

We study the optimal management of the epi-econ model in the context of two different time frames. In the first – the short-term management – the epidemic has emerged and the objective is to choose containment control, labor allocation and energy use to maximize utility. In this short time horizon, the regional natural world, temperature anomaly, and knowledge (R_i, T_i, N) are considered as fixed, since their evolution is slow relative to the the evolution of the pandemic and the primary objective is the containment of the pandemic. In this time frame, the short-term optimal controls depend parametrically on (R_i, T_i, N).

In the second – the long-term management – it is assumed that the emerged epidemic, which is the fast system, has been optimized and relaxed to a steady state which depends parametrically on the natural world R_1 and the evolution of regional temperature T_1 which is slow relative to the evolution of the epidemic and knowledge N. As (R_1, T_1, N) evolve, the short-run optimal controls for the management of the epidemic system also evolve. The relation between the epidemic system and the natural world is reflected in (10), which is the policy-independent – in the short run – component of the contact number.

For reasons explained in the introduction, we focus in the short run on noncooperative solutions in which each region maximizes own welfare. For a social optimization management problem, a social planner would maximize the global welfare indicator which could be defined as:

$$W = \log\left(Z_1^{z_1} Z_2^{z_2}\right). \tag{18}$$

The social optimization problem is examined in the long-run analysis.

3 Short-run disease containment

We study the optimal containment problem in regions $i = 1, 2$ once the epidemic has emerged. In this case the planners take the natural world $R_1(t)$, the stock of knowledge $N(t)$, and the temperature anomaly $T_1(t)$ as exogenous, and decide about the containment policy $v_i(t)$, along with labor allocation and energy use. Thus the controls for the short-run problem are $u_i = (l_{c,i}, E_{c,i}, l_{A,i}, E_{A,i}, v_i)$. The solution concept for containment policy will be a noncooperative Nash equilibrium solution in which the region's planner maximizes own regional welfare, taking the actions of the other region as given. Given that during the COVID pandemic countries have mainly been designing containment policies unilaterally though their own health systems, the Nash equilibrium concept might be a realistic representation.

3.1 Noncooperative solutions

Assuming that the objective is to contain and/or eliminate the epidemic, then the short-run time problem with fixed R_1, dropping t to ease notation, is:

$$\max_{u_i} \ln Z_i(t) \tag{19}$$

subject to

$$S_i(t) = l_{c,i} + l_{A,i} \tag{20}$$

$$\hat{S}_i(t) = \bar{\varphi}_{0i} + \varphi_{1i}\left[b_i v_i - q_j\left(1 - S_j\right)\right] \tag{21}$$

$$S_i(t) = \min\left\{\hat{S}_i, 1\right\} \tag{22}$$

$$\bar{\varphi}_{0i} = \frac{\bar{\phi}_{0i}}{1 + \varphi_{1i} m_i^{as}}, \varphi_{1i} = \frac{\phi_{1i}}{1 + \varphi_{1i} m_i^{as}}, \tag{23}$$

with $\bar{\varphi}_{0i}$ being the part of the contact number which is independent of short-term policies.

The optimality conditions for problem (19), in which infections I_{jt} in region j are taken as given, imply that:

$$v_i^* = \frac{\zeta_i \varphi_{1i} b_i}{\hat{a}_i c_{vi}} \tag{24}$$

$$\frac{\hat{a}_i a_{c,i} \beta_{l,c,i}}{l_{c,i}^*} = \frac{\hat{a}_i a_{A,i} \beta_{l,A,i}}{l_{A,i}^*} = \hat{a}_i w_{l,i} + \zeta_i \tag{25}$$

$$\frac{a_{c,i} \beta_{c,E,i}}{E_{c,i}^*} = \frac{a_{A,i} \beta_{E,A,i}}{E_{A,i}^*} = c_{E,i}, \tag{26}$$

assuming that marginal labor costs and energy costs are the same in each region for each use, and where ζ_i is the Lagrangian multiplier associated with the constraints defined by combining (20)-(22). Containment policy v_i (e.g., vaccinations) is positive as long as its effectiveness is positive and the multiplier is positive when the constraint holds as strict equality with $\hat{S}_i(t) < 1$. Condition (25) indicates that the optimal labor allocation across the two possible land uses implies equalization of marginal products, while

(26) indicates that, at the regional optimum, the marginal cost of energy equals regional marginal costs. Combining (20), (21) and (25) and solving for ζ_i, we can obtain the multiplier as a nonlinear function of S_j, or $\zeta_i = \zeta_i(S_j)$,$i, j = 1, 2$, $i \neq j$. Then the optimal containment policy can be written as:

$$v_i^* = \left(\frac{\varphi_{1i} b_i}{\hat{a}_i c_{v_i}} \right) \zeta_i(S_j) \, . \tag{27}$$

Substituting conditions (27) into (21) we obtain the nonlinear best response (or reaction) function of each region to the susceptibles of the other. The best response functions are nonlinear of the form

$$S_i \quad = \bar{\varphi}_{0i} + \varphi_{1i} \left[b_i \left(\tfrac{\varphi_{1i} b_i}{\hat{a}_i c_{v_i}} \right) \zeta_i(S_j) - q_j \left(1 - S_j\right) \right] \quad i, j = 1, 2, i \neq j. \tag{28}$$

A solution for the nonlinear system (28), if it exists, will provide the short-run optimal-containment Nash equilibrium. The system (28) is written as

$$S_i = g_i(S_j) \, , \; S_j = g_j(S_i) \tag{29}$$

$$S_i = g_i \left(g_j(S_i)\right) . \tag{30}$$

Since $S_i \in$ [0,1] and the function $g_i \left(g_j(S_i)\right)$ takes values in $[0, 1]$, the Nash equilibrium can be thought of as a fixed point of (30), since $S_i^N : S_i^N = g_i \left(g_j(S_i^N)\right)$. At the Nash equilibrium solution the susceptibles (i.e., non-infected in each region) act as strategic complements, so the containment effect in one region will help the other region. This is shown more clearly in the simulations presented in section 8. Once $\left(S_1^N, S_2^N\right)$ are obtained, then by substitution into (27) the Nash equilibrium values for the regional optimal containment policy are obtained.

Another way of looking at the short-run solution is to assume that both regions' objective is to eliminate the disease and seek control instruments $\hat{u}_i$ such that $S_i(t) = S_j(t) = 1$. The disease-eliminating instruments are obtained using (27) for $S_i(t) = S_j(t) = 1$.

Finally, we can explore the question of what the minimum size $\hat{R}_1$ is for the natural world so that a disease, if it emerges in a virus reservoir of region 1, will not spread because the contact number is below 1 (i.e., $\sigma_i(t) < 1$, $i = 1, 2$). In such a case, no containment is required and $v_{it}^* = 0$.

Using (21) and setting $S_i(t) = S_j(t) = 1$, then $\hat{R}_1$ can be defined, for any given temperature anomaly, as the minimum value of R_1 such that $(\bar{\varphi}_{0i}(R_1(t); T_1(t))) \geq 1$, since in this case $\bar{\varphi}_{0i}(R_1(t); T_1(t)) = 1/\sigma_i(t)$. We will call this value the Goodall threshold. If $R_1(t) < \hat{R}_1$ for some time t, an emerging ID will spread in at least one of the two regions and may invade the second region through transport. The containment of the disease in this case requires costly interventions.

4 Containment policy in the short run under aversion to ambiguity and model misspecification

A major issue in the design of containment policies is uncertainty regarding certain crucial parameters of the epi-econ model and concerns about misspecification of the model. Following Hansen and Miao (2018), we explore the implications of aversion to ambiguity and concerns regarding possible misspecifications of the epi-econ model from the regulators' point of view.

4.1 Robustness and entropy penalization

Assume that a parameter ν of the epi-econ model, such as b_i, u_i, φ_{0i}, or φ_{1i}, $i = 1, 2$, has a prior density π, with $\nu \in \mathcal{V}$. In the context of Hansen and Miao's (2018) approach to ambiguity and model misspecification aversion, the regulator solves the problem:

$$\max_{u_i(t)} \min_{\pi} \int_{\mathcal{V}} U_i(C_i; \nu)\, \pi(\nu)\, d\nu + \kappa_i \int_{\mathcal{V}} [\log \pi(\nu) - \log \hat{\pi}(\nu)]\, \pi(\nu)\, d\nu, \quad (31)$$

where $u_i = (l_{c,i}, E_{c,i}, l_{A,i} E_{A,i}, v_i)$. In (31), aversion to ambiguity and model misspecification is modeled by introducing a fictitious adversarial or minimizing agent (MA) who distorts the baseline prior density of an uncertain parameter, in order to impose a cost on the regulator who is the maximizing agent. This cost reflects the impact of aversion to uncertainty and model misspecification. By designing regulation based on (31), the regulator derives a decision rule which incorporates this aversion.

In (31), $\hat{\pi}(\nu)$ is the baseline density for the parameter ν, and $\kappa > 0$ is a parameter which penalizes deviations from the baseline density $\hat{\pi}(\nu)$ with $\int_{\mathcal{V}} [\log \pi(\nu) - \log \hat{\pi}(\nu)]\, \pi(\nu)\, d\nu$ being the relative entropy discrepancy from the baseline density. For $\kappa \to \infty$, the regulator is committed to the baseline density, which can be interpreted as the case in which – when the cost of distorting the prior to the MA is infinite – the decision making is using the baseline. As $\kappa \to 0$, the distortion tends to the worst case prior. In problem (31), the regulator maximizes utility using the controls of the epi-econ model, while Nature, acting as the MA, distorts the baseline prior density of parameters associated with the controls. The regulator is concerned about the distortion of the prior of the epi-econ model parameters and follows robust control regulation. The solution of the minimization part of problem (31) is given (see Hansen and Miao 2018) as:

$$\pi^* (\nu) = \frac{\exp\left[-\frac{1}{\kappa} U_i (C_i; \nu)\right] \hat{\pi}(\nu)}{\int_{\mathcal{V}} \exp\left[-\frac{1}{\kappa} U_i (C_i; \nu)\right] \hat{\pi}(\nu)\, d\nu}. \tag{32}$$

Substituting $\pi^* (\nu)$ into (31), the objective to be maximized by the regulator becomes

$$J_i = \max_{u_i(t)} \left\{ -\kappa \log \int_{\mathcal{V}} \exp\left[-\frac{1}{\kappa} U_i (C_i; \nu)\right] \hat{\pi}(\nu)\, d\nu \right\}. \tag{33}$$

We set $\theta = 1/\kappa$ and interpret θ as the robustness parameter. When $\theta \to 0$ ($\kappa \to \infty$), the regulator optimizes using the baseline prior; when $\theta \to \infty$ ($\kappa \to 0$), the regulator optimizes by taking into account the worst case prior. Expanding (33) around $\theta = 0$ and using the cumulant generating function, we obtain the expansion

$$K_i (\theta, \nu) = \mathbb{E}_{\hat{\pi}} \left[U_i (C_i; \nu)\right] - \frac{\theta}{2} \mathrm{Var}_{\hat{\pi}} \left[U_i (C_i; \nu)\right]. \tag{34}$$

Assume for the stochastic parameter that $\nu \in \mathcal{V} = \left[\underline{\nu}, \bar{\nu}\right]$ with mean μ_ν and variance σ_ν^2 in the baseline density. Expanding the $K_i (\theta, \nu)$, we obtain:

$$\mathbb{E}_{\hat{\pi}} \left[U_i (C_i; \nu)\right] \approx U_i (C_i; \mu_\nu) + \frac{U_i'' (C_i; \mu_\nu)}{2} \sigma_\nu^2 \tag{35}$$

$$\mathrm{Var}_{\hat{\pi}} \left[U_i (C_i; \nu)\right] \approx \left(U_i' (C_i; \mu_\nu)\right)^2 \sigma_\nu^2, \tag{36}$$

where the derivatives of the utility function are taken with respect to the stochastic parameter ν. Then the maximization problem for the regulator in region i becomes

$$J_i = \max_{u_i(t)} \left\{ U_i\left(C_i;\mu_\nu\right) + \frac{U_i''\left(C_i;\mu_\nu\right)}{2}\sigma_\nu^2 - \frac{\theta}{2}\left(U_i'\left(C_i;\mu_\nu\right)\right)^2\sigma_\nu^2 \right\}. \tag{37}$$

If we disregard second-order terms, the optimization problem described by (37) suggests that the utility of the decision maker is penalized by a term defined by the marginal utility of a small change in the mean of the ambiguous parameter by the variance of the baseline prior and the robustness parameter θ. When $\theta \to 0$, the decision maker is an expected utility maximizer and uses the baseline prior.

4.2 Regulation under aversion to ambiguity

Keeping regional T_1 and R_1 fixed, we study the impact of increasing the robustness parameter θ on the optimal choice of controls by comparative statics. Increasing the robustness parameter θ means that regulation takes into account distorted priors which deviate from the baseline and, at the limit as $\theta \to \infty$, they tend to the worst case scenario. Regulation under aversion to ambiguity implies that after disregarding R_1, T_1 which are constants in the short run, and then using (33) after replacing κ with $1/\theta$, the objective of the regulator in region $i = 1, 2$ for the noncooperative case becomes

$$J_i = \max_{u_i(t)} \left\{ \hat{a}_i \log C_i - \frac{1}{\theta}\ln\left(\mathbb{E}\exp\left[\left(-\theta\right)\zeta_i\varphi_{1i}b_iv_i\right]\right) \right\}, \tag{38}$$

subject the constraints of problem (19). The first-order conditions for the optimal containment policy v_i imply

$$v_i^* = \frac{1}{\hat{a}_i c_{v_i}} \frac{\mathbb{E}\exp\left[\left(-\theta\right)\zeta_i(S_i)\varphi_{1i}b_iv_i\right]\zeta_i(S_i)\varphi_{1i}b_i}{\mathbb{E}\exp\left[\left(-\theta\right)\zeta_i(S_i)\varphi_{1i}b_iv_i\right]} = g\left(\theta, v_i; \zeta_i\right). \tag{39}$$

Proposition 1. *Consider the epi-econ model (19) and assume that the parameter b_i, which reflects the effectiveness of the containment control, is uncertain with a baseline prior $\hat{\pi}\left(b_i\right)$. Then the Nash equilibrium under ambiguity can be defined, while an increase in the robustness parameter θ will reduce containment policy in region i.*

For the proof, see Appendix.

Since the ambiguous parameter is on the effectiveness of control efforts against the emerging ID (that is, b_i), if the worst case value of b_i is zero, then when it costs zero for the adversarial agent to harm the regulator through the ambiguous parameter b_i, the best reply of the regulator in the zero sum game is to set $v_i^* = 0$. The intuition is that as θ increases and the aversion of the regulator induces him/her to consider distorted priors regarding the effectiveness or the cost of the containment policy which are worse relative to the baseline, less control is exercised, since its effectiveness tends to zero in the worst case scenario. Since the setup can be generalized to a vector of controls represented by a linear combination of specific controls determining containment policy (that is, $b_i v_i = \sum_{j=1}^{J} b_{ij} v_{ij}$, $i = 1, 2$), Proposition 1 suggests that high aversion to ambiguity regarding the effectiveness of a specific control will reduce the use of this control and will potentially increase the use of other controls which are less ambiguous.

4.3 Strong preferences for robustness and ambiguity-adjusted Nash equilibrium

Optimal containment policies can be obtained by maximizing (94) and using first-order condition (95) from the proof of Proposition 1 in section 9.1 of the Appendix for the optimal choice of v. To simplify, assume that the baseline prior for the effectiveness of parameter b_i is a uniform distribution with

$$\begin{aligned} b_i &\in [m_{b_i}, M_{b_i}], 0 \leq m_{b_i} \leq M_{b_i} \\ \hat{\mu}_{b_i} &= \frac{m_{b_i} + M_{b_i}}{2}, \hat{\sigma}^2_{b_i} = \frac{(M_{b_i} - m_{b_i})^2}{12}. \end{aligned}$$

Using this assumption in (94) and the moment-generating function of the uniform distribution, we obtain

$$\frac{-1}{\theta} \ln \left(\mathbb{E} \exp\left[(-\theta)\, \varphi_{1i} b_i v_i\right]\right) =$$
$$\frac{-1}{\theta} \log \left(\frac{\exp\left[(-\theta)\, \varphi_{1i} \zeta_i M_{b_i} v_i\right] - \exp\left[(-\theta)\, \varphi_{1i} \zeta_i m_{b_i} v_i\right]}{\theta \varphi_{1i} M_{b_i} v_i - \theta \varphi_{1i} m_{b_i} v_i} \right) = h\left(\theta, v_i\right)$$

with

$$\lim_{\theta \to \infty} h\left(\theta, v_i\right) = \varphi_{1i} \zeta_i m_{b_i} v_i \ , \ \lim_{\theta \to 0} h\left(\theta, v_i\right) = \varphi_{1i} \zeta_i \hat{\mu}_{b_i} v_i.$$

Thus when $\theta \to \infty$, the regulator is infinitely robust and uses the worst case scenario, while when $\theta \to 0$, the regulator uses the baseline prior. With b-ambiguity, the optimal control for the worst case is

$$v_i^{a,w} = \left(\frac{\varphi_{1i} m_{b_i}}{c_{v_i}}\right) \zeta_i(S_j) \,. \tag{40}$$

Considering the b-ambiguity case, the best response function at a fixed time t is defined as:

$$S_i \quad = \bar{\varphi}_{0i} + \varphi_{1i}\left[b_i\left(\tfrac{\varphi_{1i} m_{b_i}}{c_{v_i}}\right)\zeta_i(S_j) - q_j\left(1 - S_j\right)\right] \quad i, j = 1, 2, i \neq j. \tag{41}$$

Since $m_{b_i} < \hat{\mu}_{b_i}$, the worst case prior for the policy effectiveness implies less control relative to the baseline prior at the Nash equilibrium. The impact of increased aversion to ambiguity regarding the effectiveness of containment policies is a shift of the best response functions towards the origin which implies an increase in the Nash equilibrium share of infected. This is presented and verified by the numerical simulations in section 7.1.

Thus ambiguity regarding the effectiveness of containment measures leads, in a Nash equilibrium, to an increase in the share of infected. The effectiveness of containment measures could be related to technical characteristics such as weak effectiveness of vaccines but also to social characteristics such as opposition to social distancing or vaccination. Reduced vaccinations and opposition to containment measures in parts of the world during the COVID pandemic could suggest increased ambiguity regarding the vaccinations associated with the containment policy v.

Consider now the case where the regulator of a region expresses aversion to ambiguity regarding $\bar{\varphi}_{0i}$, the part of the contact number that does not depend on short-run policies. Then from (94) the regulator's problem for region i can be written as

$$J_i = \max_{u_i(t)} \left\{ \log C_i - \frac{1}{\theta} \ln\left(\mathbb{E} \exp\left[\left(-\theta_i \zeta_i \bar{\varphi}_{0i}\right)\right]\right) \right\}.$$
$$\zeta_i = \zeta_i(S_i^N).$$

Assume that the baseline prior for the policy-independent part of the contact number is a uniform distribution with the worst case being $\bar{\varphi}_{0i} = 0$, and parameters in the following intervals:

$$\begin{aligned}\bar{\varphi}_{0i} &\in [0, M_i] \\ \hat{\mu}_i &= \frac{M_i}{2}, \hat{\sigma}_i^2 = \frac{(M_i)^2}{12}.\end{aligned}$$

Then, using the moment-generating function for the uniform distribution, we obtain

$$h_i(\theta) = -\frac{1}{\theta}\log\left(\mathbb{E}\exp\left[(-\theta\bar{\varphi}_{0i})\right]\right) = -\frac{1}{\theta}\log\left(\frac{\exp\left[(-\theta)\zeta_i M_i\right]-1}{\theta\zeta_i M_i}\right).$$

If the regulator in region i is infinitely robust, then $\lim_{\theta\to\infty} h(\theta) = 0$. This means that if aversion to ambiguity regarding the effectiveness of the short-run containment measures b_i tends also to infinity and the worst case is associated with $m_{b_i} = 0$, then as verified by our numerical simulations the inverse of the contact number

$$\hat{S}_i = \frac{1}{\sigma_i} = \bar{\varphi}_{0i} + \varphi_{1i}\left[b_i\left(\frac{\varphi_{1i}m_{b_i}}{c_{v_i}}\right)\zeta_i(S_j) - q_j(1-S_j)\right] \to 0,$$

which implies that at the limit the whole population will be infected in the Nash equilibrium. This observation leads to the following claim:

Claim: *When the ambiguity of the regulator about the policy-independent parameter (which is uniformly distributed on $[0, M_i]$) in the short-run component of the contact number is very high, that is, $\theta \to \infty$, so the regulator optimizes by taking into account the worst case prior, the only route for reducing the contact number is to reduce ambiguity about the effectiveness of the short-run containment policy, i.e., reduce ambiguity on "b". When this short-run ambiguity cannot be reduced for voluntary-based containment policies, supplementary policies, such as for example fines for non-compliers, might be necessary.*

Consider now the case in which in region i, say $i = 1$, the worst cases for $\bar{\varphi}_{01}$ and b_1 imply at the limit that $\hat{S}_1 \to 0$. In this case the optimizing region $j = 2$ will not respond to region 2's choices but will unilaterally adopt containment control policies. The optimal containment policy for this region will be:

$$v_2^{a,w} = \frac{\varphi_{2j}\hat{\mu}_{b_2}}{c_{v_2}}\zeta_2(S_2).$$

In this case the equilibrium susceptibles in region 2 will be the fixed point of

$$S_2 = \frac{1}{\sigma_2} = \bar{\varphi}_{02} + \varphi_{12}\left[b_i\left(\frac{\varphi_{2j}\hat{\mu}_{b_2}}{c_{v_2}}\zeta_2(S_2)\right)\zeta_2(S_2) - q_j\right].$$

The result is confirmed by simulation which suggests zero susceptibles for one region and a slight drop in the susceptibles of the other region relative to the no-ambiguity Nash equilibrium. This result could explain differences in infection and policy effectiveness across regions observed during the COVID-19 pandemic.

4.3.1 A generalization

To more clearly provide a picture of the noncooperative equilibrium between the two regions for more general baseline priors, we use approximations (34)-(37) and consider ambiguity in the effectiveness of the containment policy, b_i, $i = 1, 2$. Applying (34)-(37), we consider the problem:

$$J_i = \max_{u_i(t)}\left\{\hat{a}_i \log C_i - \frac{\theta}{2}\hat{\sigma}^2_{b_i}\left(\zeta_i\varphi_{1i}v_i\right)^2\right\},$$

subject to the constraints of problem (19) where ζ_i is the Lagrangian multiplier of constraint (20). The optimality condition implies

$$v_i^{*a} = \frac{\zeta_i(S_i^N)\varphi_{1i}\hat{\mu}_{b_i}}{c_i + \theta_{b_i}\left(\zeta_i(S_i^N)^2\hat{\sigma}_{b_i}\varphi_{1i}\right)^2}, \quad (42)$$

where $\hat{\mu}_{b_i}, \hat{\sigma}^2_{b_i}$ are the mean and variance of the baseline prior for ambiguous parameters corresponding to the effectiveness of the containment policy. If we assume that the baseline prior is uniform with $b_i \in [m_{b_i}, M_{b_i}]$, $0 \leq m_{b_i} \leq M_{b_i}$, then (42) can be further simplified by setting $\hat{\mu}_{b_i} = \frac{m_{b_i}+M_{b_i}}{2}$, $\hat{\sigma}^2_{b_i} = \frac{\left(M_{b_i}-m_{b_i}\right)^2}{12}$.

Along the lines of Proposition 1, differences across regions in concerns regarding the effectiveness of instruments in reducing the contact number differentiate the optimal values for the containment instruments. The region for which ambiguity about the effectiveness of a costly instrument is stronger will use less of this instrument relative to a region in which ambiguity about the effectiveness of the instrument is relatively smaller. This result can differentiate between containment policies which are based on voluntary behavior only, versus menus of policies. If the introduction of supplementary policies such as fines for non-compliers is characterized by less ambiguity, it will be used along with voluntary containment policies. Thus ambiguity differentials differentiate the optimal intensity of use of the containment policies and introduce policy trade-offs. Furthermore, in line with the theory, as $\theta \to 0$ the optimal controls are designed on the baseline prior, while if regulation is designed on the basis of the worst case regarding the effectiveness of the control and $\theta \to \infty$, then no control is undertaken.

5 Disease prevention in the long run: climate change, natural world preservation and innovation

In the previous section we studied disease containment in the short run by assuming that the disease has already emerged and that the infected-susceptible dynamics move fast towards their steady-state values. In the short run, the allocation of the regional land between agriculture and preservation, and the regional temperature anomalies, were treated as exogenous parameters. In the long run, however, land use can change, while temperature will evolve responding to the use of fossil fuels and climate policies. Changes in land use which might reduce the natural world and bring human activities closer to disease reservoirs, along with an increase in regional average temperatures, will affect the long-run path of the contact rate φ_{0i}, which is basically independent of short-term containment policies.

5.1 Noncooperative long-run prevention

To study noncooperative solutions in the long run, we assume that each region takes as given the initial temperature anomaly and the initial stock of knowledge and commits to the emission and innovation paths (region 2 only) that optimize own welfare functions, given the best response of the other region. The solution of this problem will characterize an open loop Nash equilibrium (OLNE). The consumption flow for the slow time scale problem is obtained by substituting the fast-time (short-run) optimal controls for containment v_i^* into $\hat{S}_i$ to obtain the short-run Nash equilibrium levels of susceptibles S_i^N. Then the control problem for region i in the time scale of the climate change can be written as:

$$J_i^N = \max_{\{u_i(t), R_i(t), n_i(t)\}} \int_0^{\infty} \mathrm{e}^{-\rho t} \left[\hat{a}_i \ln C_i(t) + \hat{b}_i \ln R_i(t) \right] dt, \tag{43}$$

subject to (5)-(7) and (20)-(23), with $\rho > 0$ the utility discount rate, with controls

$$\mathbf{u}_i(t) = \left(l_{c,i}(t), l_{A,i}(t), L_{A,i}(t), E_{c,i}(t), E_{A,i}(t), n_2(t) \right),$$

and states

$$\mathbf{x} = (X, N).$$

In this optimization problem, after dropping t to ease notation, the following constraints apply:

$$\hat{S}_i = \varphi_{0i}(R_1, T_1) + \varphi_{1i} \left[b_i v_i^* \left(S_i^N \right) - q_j \left(1 - S_j^N(t) \right) \right] \tag{44}$$

$$S_i = \min \left\{ \hat{S}_i, 1 \right\} \tag{45}$$

$$\varphi_{0i}(R_1, T_1) = \frac{\phi_{it}(R_1, T_1)}{1 + \phi_{1i} m_i^{as}}, \varphi_{1i} = \frac{\phi_i}{1 + \varphi_{1i} m_i^{as}} \tag{46}$$

$$R_i = \bar{L}_i - L_{A,i} \tag{47}$$

$$S_i = l_{c,i} + l_{A,i} \tag{48}$$

$$E_i = E_{c,i} + E_{A,i} \tag{49}$$

$$T_i(t) = \Lambda_i X(t), \tag{50}$$

where $\varphi_{1i} \left[b_i v_i^* \left(S_i^N \right) - q_j \left(1 - S_j^N \right) \right] = \bar{\varphi}_{1i}$ is fixed at the solution of the short-run problem and aggregate regional energy or, equivalently, use of GHGs is $E_i = E_{c,i} + E_{A,i}$. Each region takes the action paths of the other region as fixed and solves problem (43). The current value Lagrangians for the problem of each region can be defined as:

$$\mathcal{L}_1 = \mathcal{H}_1 + \kappa_1 \left[\varphi_{01} \left(\bar{L}_1 - L_{A,1}, T_1 \right) + \bar{\varphi}_{11} - l_{c,1} - l_{A,1} \right] \tag{51}$$

$$\mathcal{H}_1 = \left[\hat{a}_1 \ln C_1 + \hat{b}_1 \ln \left(\bar{L}_1 - L_{A,1} \right) \right] + \lambda_1 \left[E_1(t) + E_2(t) - dX \right] \tag{52}$$

and

$$\mathcal{L}_2 = \mathcal{H}_2 + \kappa_2 \left[\varphi_{02}\left(\bar{L}_1 - L_{A,1}, T_1\right) + \bar{\varphi}_{12} - l_{c,2} - l_{A,2}\right] \tag{53}$$

$$\begin{aligned} \mathcal{H}_2 = &\left[\hat{a}_2 \ln C_2 + \hat{b}_2 \ln\left(\bar{L}_2 - L_{A,2}\right)\right] + \lambda_2\left[E_1(t) + E_2(t) - dX\right] \\ &+ \xi_2\left[n_2(t) - mN\right], \end{aligned} \tag{54}$$

where $\mathcal{H}_i$ are the regional current value Hamiltonians. The Lagrangian multipliers, κ_i, should be interpreted as the sensitivity of the optimal solution to changes in the constrained constants. The costate variable λ_i has the usual interpretation as the shadow cost of the GHGs accumulation or the regional social cost of carbon (SCC), while the costate variable ξ_2 has the interpretation of the shadow value of innovation in the industrial agricultural sector. A solution of problem (43), if it exists, will characterize the OLNE.

The problem represented by (51)-(54) provides the link for the epi-econ model. An increase in the use of agricultural land will have a positive impact on regional welfare because it will increase the consumption aggregate and a negative impact because it will increase the contact rate and reduce Nature's input through the reduction in R_i. In this model the impact of accumulated land augmenting knowledge in, say bioengineering, can be understood in the following way.

Remark 1. Consider a steady state of (43) without any agricultural land augmenting innovation, or $\left(L^*_{A,1}, N^* = 1\right)$ and a steady state with land augmenting innovation $\left(L^{*A}_{A,1}, N^{*A} > 1\right)$. If

$$\left(N^{*A} L^{*A}_{A,1} \geq L^*_{A,1}, L^{*A}_{A,1} < L^*_{A,1}\right),$$

then at the "with innovation" steady state, Nature R_1 increases in the region which is an ID hot spot. This could reduce Nature's impact on long-run ID intensity. Whether an overall reduction in the contact rate takes place depends on the evolution of fossil fuel use and climate change. Knowledge accumulation will be beneficial in each region if $\max J_i^{NA} > \max J_i^N, i = 1, 2$, where $\max J_i^{NA}$ stands for maximized welfare under land augmenting innovation. It should be noted that the assumption that knowledge is accumulated in the North and diffuses freely to the tropics benefits both regions in terms of ID.

5.1.1 Optimality conditions

Problem (43) as represented by (51)-(54) is an optimal control problem with mixed constraints. The optimality conditions (e.g., Seierstad and Sydsaeter 1986, chapter 4) can be written, under the assumption of interior solutions for the controls to ease exposition, as:

$$\frac{\hat{a}_i a_{c,i} \beta_{l,c,i}}{l_{c,i}} = \frac{\hat{a}_i a_{A,i} \beta_{l,A,i}}{l_{A,i}} = \kappa_i + \hat{a}_i w_{l,i} \tag{55}$$

$$\frac{\hat{a}_i a_{c,i} \beta_{c,E,i}}{E_{c,i}} = \frac{\hat{a}_i a_{A,i} \beta_{A,E,i}}{E_{A,i}} = \hat{a}_i c_{E_i} - \lambda_i \tag{56}$$

$$\frac{\hat{a}_1 a_{A,1} \beta_{L,A,1}}{L_{A,1}} = \hat{a}_1 c_{L,1} + \kappa_1 \frac{\partial \varphi_{01}}{\partial \left(\bar{L}_1 - L_{A,1} \right)} + \frac{\hat{b}_1}{\bar{L}_1 - L_{A,1}} \tag{57}$$

$$\frac{\hat{a}_2 a_{A,2} \beta_{L,A,2}}{L_{A,2}} = \hat{a}_2 c_{L,2} + \frac{\hat{b}_2}{\bar{L}_2 - L_{A,2}} \tag{58}$$

$$\dot{\lambda}_i = (\rho + d) \lambda_i + \hat{a}_i \omega_i \Lambda_i^2 X + \kappa_i \frac{\partial \varphi_{0i}(R_1, T_1)}{\partial T_1} \tag{59}$$

$$\dot{X} = E_1^* + E_2^* - dX \tag{60}$$

$$E_i^* = \frac{\Gamma_i}{\hat{a}_i c_{E_i} - \lambda_i} \tag{61}$$

$$\Gamma_i = \hat{a}_i \left(a_{c,i} \beta_{c,E,i} + a_{A,i} \beta_{E,A,i} \right) \tag{62}$$

$$n_2^* = \frac{\xi_2}{\hat{a}_2 c_{n_2}} \tag{63}$$

$$\dot{\xi}_2 = (\rho + m) \xi_2 - \frac{\hat{a}_2 a_{A,2} \beta_{L,A,2}}{N} \tag{64}$$

$$\dot{N} = n_2^* - mN. \tag{65}$$

5.1.2 Discussion of the optimality conditions

Labor allocation conditions (55) indicate that the marginal product of labor in all uses equals the shadow value of an additional non-infected labor unit plus any marginal labor costs. Energy use in all uses equates the marginal energy cost plus the regional SCC as shown in (56). The aggregate energy flow from each region is given by (61). For land allocation, (57) indicates that in region 1 – the ID hot spot – the marginal product of land allocated to industrial agriculture, defined in terms of effective land ($NL_{A,1}$), should be equal to marginal land-use costs plus the shadow value of total available land in the region weighted by the impact of increasing the use of agricultural land by a small amount on the contact number, plus the marginal cost in terms of reducing Nature's services. Note that the stock of knowledge is decided by the North through (63)-(65). The impact of land augmenting knowledge can be further clarified with the help of figure 1.

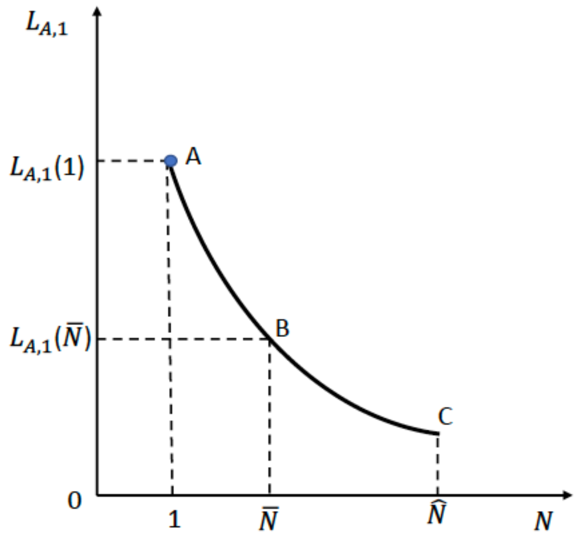

Figure 1: The impact of land augmenting technology.
Point A corresponds to an agricultural land allocation without any knowledge accumulation ($N = 1$). The line AC defines land use as

$$L_{A,1}(N) = \frac{L_{A,1}(1)}{N},\ N \in [1, \hat{N}].$$

Suppose that knowledge accumulation increases to $\bar{N}$. Then land use can be reduced to $L_{A,1}(\bar{N})$ with an equivalent increase of land left to Nature, while the effective land input is the same as $L_{A,1}(1)$. This reduces the contact rate in both regions as indicated by (10) and increases ecosystems' contribution to the composite good.

Finally, the cost of climate change is governed by (59) which describes the evolution of the SCC. It can be seen that this social cost in addition to climate change damages includes which impact of temperature on the contact number weighted by the regional TCRE.

5.1.3 Policy implications

Optimality condition (57) suggests that the cost of converting one unit of Nature to industrial agriculture consists of two parts. The first is the loss in ecosystem services $\frac{\hat{b}_1}{L_{A,1}}$ which is the traditional concept used in cost-benefit analysis of conversion vs preservation and in valuations studies such as contingent valuation. The second represents a new type of cost emerging from the epi-econ model which reflects the cost in terms of emerging ID associated with the reduction of the natural world in order to increase industrial agriculture, $\kappa_1 \frac{\partial \varphi_{01}}{\partial L_{A,1}}$.

Condition (59) suggests that SCC should include, in addition to the standard concept of damages to the economy – $\hat{a}_i \omega_i \Lambda_i X$, in this case – the extra cost in terms of emerging IDs, $\kappa_i \frac{\partial \varphi_{0i}(R_1,T_1)}{\partial T_1} \omega_1$, induced by a unit of GHG emissions. This extra cost should be taken into account in carbon pricing.

5.1.4 The OLNE steady state: knowledge

The dynamics of the knowledge subsystem decouple from the dynamics of the climate subsystem. This is because the structure of the problem – which is logarithmic in (NL) along with linear dynamics for knowledge accumulation – makes the optimal R&D flow depend on the shadow value of knowledge only, as indicated by (63)-(65). Then, the steady state is defined as:

$$N = \frac{\xi_2}{\hat{a}_2 c_{n_2} m} \tag{66}$$

$$\xi_2 = \frac{\hat{a}_2 a_{A,2} \beta_{L,A,2}}{(\rho + m) N} \tag{67}$$

or

$$\begin{aligned} \xi_2^{\infty} &= \left(\frac{\hat{a}_2^2 a_{A,2} \beta_{L,A,2} c_{n_2} m}{(\rho + m)} \right)^{1/2} \\ N^{\infty} &= \frac{\xi_2^*}{\hat{a}_2 c_{n_2} m}. \end{aligned} \tag{68}$$

Proposition 2. *The steady state (ξ_2^*, N^*) for knowledge accumulation exists, it is unique and a saddle point.*

For the proof, see Appendix.

The convergence to the steady state is shown in figure 5.

5.1.5 The OLNE steady state: climate

To study the Hamiltonian system (59)-(61) which determines the OLNE for climate, we need to define the optimal controls as functions of the state-costate variables (T_i, λ_i). In order to provide a clear picture of the structure and the properties of this steady steady state – given the nonlinearity of the optimality conditions for the controls (55)-(58) – we consider a linearization of these conditions, say around the short-run Nash equilibrium, and we assume a linear representation of the inverse of the contact number for the part that depends on Nature and climate, or:

$$\varphi_{0i}\left(R_1, T_1\right) = \gamma_{0i} + \gamma_{iR_i}\left(\bar{L}_1 - L_{A,1}\right) - \gamma_{iT_1} T_1. \tag{69}$$

Solving the linearized first-order conditions for the controls in terms of the multipliers κ_i for (55) and (57) and the costate variables λ_i for (56); substituting the solutions into the constraints associated with the multipliers κ_i; solving for κ_i and substituting the solutions back into (55) and (57), we obtain the land allocation as a function of temperature in region 1 and accumulated knowledge, while energy use is directly related to the regional SCC through (56). These conditions represent the feedback controls for land-labor allocation, energy use and natural world preservation as functions of climate change, the productivity of the economy, the exogenous land availability and the short-term disease-containment parameter. The evolution of the OLNE potentially towards a steady state can be studied by substituting the feedback controls into (59)-(60).

5.1.6 Open loop Nash equilibrium

Since the knowledge system decouples for the climate system, each region replies optimally on the other region's emissions as indicated by (61), and the reply depends only on the region's shadow cost of GHG $\lambda_i(t)$. The regions are not symmetric, therefore their corresponding shadow costs of GHG are expected to be different, $\lambda_1(t) \neq \lambda_2(t)$, while the state variable $X(t)$ is common for both regions. Therefore the OLNE for the climate subsystem should be analyzed in the context of a three-dimensional Hamiltonian system describing the evolution in time of $(X(t), \lambda_1(t), \lambda_2(t))$.

Proposition 3. *There is a unique OLNE steady state* $\mathbf{x}^{\infty} = (\lambda_1^{\infty}, \lambda_2^{\infty}, X^{\infty})$ *for the two-region linearized system with the saddle point property.*[12]

[12] We study the properties of the long-run open loop Nash equilibrium in the neighborhood of the short-run "static" Nash equilibrium. This seems to be reasonable if an emerging ID has been controlled and the regions or a social planner, as we shall see later, after recognizing the importance of land-use and climate change in IDs, seeks long-run optimal policies. The behavior of the full nonlinear system from any initial state and the possibility of multiple steady states should be an area of further study.

For the proof, see Appendix.

The OLNE steady state can be used to determine the corresponding OLNE steady states for the controls for labor, land, energy and the natural world. In particular the solutions $(\lambda_1^\infty, \lambda_2^\infty)$ can be used to determine energy from the linearized version of (56). The solution for $T_i^\infty = \Lambda_i X^\infty$ can be used to determine (κ_1^*, κ_2^*) and then labor use and agricultural land use through the linearized versions of (55), (57). Then the natural world can be obtained as $R_i^\infty = \bar{L}_i - L_i^\infty$.

Proposition 3 suggests that the regional SCC, and therefore any climate policy based on this concept, should include an additional component related to the impact of climate change on the contact number of the emerging ID. This component is reflected in the term $\kappa_i^* \gamma_{2T_1} \Lambda_1$. The positivity of the term κ_i^* is reasonable because it implies that optimal containment policy in the very short run will improve the overall performance of the system, since this term reflects the sensitivity of the optimal solution to a small change in the short-run optimal containment parameter.

The saddle point stability implies that for any initial value of GHGs in the neighborhood of the steady state, the OLNE paths converging to this steady state can be approximated as:

$$X(t) = A_1 c_{11} e^{-\varrho_1 t} + X^\infty \, , X(0) = X_0 \tag{70}$$

$$\lambda_1(t) = A_1 c_{21} e^{-\varrho_1 t} + \lambda_1^\infty \tag{71}$$

$$\lambda_2(t) = A_1 c_{31} e^{-\varrho_1 t} + \lambda_2^\infty , \tag{72}$$

where the parameters (A, c, ϱ) are calculated at the solution using the appropriate eigenvector and the initial value for the GHG stock, with $-\varrho_1$ the negative eigenvalue. Note that the system evolves in three-dimensional state-costate space because the differential game is asymmetric. Substitution of the paths (70)-(72) into the corresponding optimality conditions for the controls will determine the OLNE time paths for the controls which will drive the system to the OLNE steady state. Convergence to the steady state in the three-dimensional state-costate space is shown in figure 3.

6 The long-run social optimum

To attain the social optimum a social planner maximizes a social welfare function of the form $\log\left(Z_1^{z_1} Z_2^{z_2}\right)$, subject to the relevant constraints. The planner's current value generalized Hamiltonian is:

$$\begin{aligned}\mathcal{H} = z_1 \left[\hat{a}_1 \ln C + \hat{b}_1 \ln\left(\bar{L}_1 - L_{A,1}\right)\right] + z_2 \left[\hat{a}_2 \ln C_2 + \hat{b}_2 \ln\left(\bar{L}_2 - L_{A,2}\right)\right] + \\ \lambda\left[E_1(t) + E_2(t) - dX\right] + \xi_2\left[n_2(t) - mN\right] + \\ \kappa_1\left[\varphi_{01}\left(\bar{L}_1 - L_{A,1}, T_1\right) + \bar{\varphi}_{11} - l_{c,1} - l_{A,1}\right] + \\ \kappa_2\left[\varphi_{02}\left(\bar{L}_1 - L_{A,1}, T_1\right) + \bar{\varphi}_{12} - l_{c,2} - l_{A,2}\right],\end{aligned} \tag{73}$$

with optimal conditions, assuming interior solutions for the controls:

$$\frac{z_i \hat{a}_i a_{c,i} \beta_{l,c,i}}{l_{c,i}} = \frac{z_i \hat{a}_i a_{A,i} \beta_{l,A,i}}{l_{A,i}} = \kappa_i + z_i \hat{a}_i w_{l,i} \tag{74}$$

$$\frac{z_i \hat{a}_i a_{c,i} \beta_{c,E,i}}{E_{c,i}} = \frac{z_i \hat{a}_i a_{A,i} \beta_{A,E,i}}{E_{A,i}} = z_i \hat{a}_i c_{E_i} - \lambda \tag{75}$$

$$\frac{z_1 \hat{a}_1 a_{A,1} \beta_{L,A,1}}{L_{A,1}} = z_i \hat{a}_1 c_{L,1} + \frac{\kappa_1 \partial \varphi_{01}}{\partial\left(\bar{L}_1 - L_{A,1}\right)} + \frac{z_1 \hat{b}_1}{\left(\bar{L}_1 - L_{1A,1}\right)} + \frac{\kappa_2 \partial \varphi_{02}}{\partial\left(\bar{L}_1 - L_{1A,1}\right)} \tag{76}$$

$$\frac{\hat{a}_2 a_{A,2} \beta_{L,A,2}}{L_{A,2}} = \hat{a}_2 c_{L,2} + \frac{\hat{b}_2}{\left(\bar{L}_2 - L_{A,2}\right)} \tag{77}$$

$$\dot{\lambda} = (\rho + d)\lambda + \sum_{i=1,2} z_i \hat{a}_i \omega_i \Lambda_i^2 X + \sum_{i=1,2} \kappa_i \frac{\partial \varphi_{0i}(R_1, \Lambda_1 X)}{\partial X} \tag{78}$$

$$\dot{X} = E_1^* + E_2^* - dX \tag{79}$$

$$E_i^* = \frac{\Gamma_i}{z_i \hat{a}_i c_{E_i} - \lambda} \tag{80}$$

$$\Gamma_i = z_i \hat{a}_i \left(a_{c,i} \beta_{c,E,i} + a_{A,i} \beta_{A,E,i}\right) \tag{81}$$

$$n_2^* = \frac{\xi_2}{\hat{a}_2 z_2 c_{n_2}} \tag{82}$$

$$\dot{\xi}_2 = (\rho + m)\xi_2 - \sum_{i=1,2} \frac{z_i \hat{a}_i a_{A,i} \beta_{L,A,i}}{N} \tag{83}$$

$$\dot{N} = n_2^* - mN. \tag{84}$$

6.1 Discussion of the optimal conditions and policy implications

Optimality conditions for labor allocation and energy use, (74) and (75) respectively, have the same structure as the optimality conditions for the noncooperative solution but with an adjustment for the welfare weights (z_1, z_2), while the shadow cost of GHGs in energy use is now the global SCC and not the regional one. The socially optimal land allocation for agriculture in region 1, (76), takes into account, relative to the noncooperative allocation rule, the ID cost induced in region 2 by reducing the natural world in region 1 in order to increase agricultural land in region 1. This is represented by the term $\frac{\kappa_2 \partial \varphi_{02}}{\partial\left(\bar{L}_1 - L_{1A,1}\right)}$. The SCC, which is the solution of (78), contains two additional terms relative to the noncooperative solution. The term $\sum_{i=1,2} z_i \hat{a}_i \omega_i \Lambda_i X$ represents global economic damages from GHGs. The term $\sum_{i=1,2} \kappa_i \frac{\partial \varphi_{0i}(R_1, \Lambda_1 X)}{\partial X}$ is the global ID cost attributed to the SCC since an increase in the GHGs will have a positive effect on the contact number of IDs emerging in region 1 and affecting region 2 as well. Finally, (83) indicates that the shadow value of knowledge accumulation should take into account the impact of knowledge in both regions.

These results suggest that in order to correct the distortions of the noncooperative solution and try to attain the global social optimum, three distortions should be corrected: the land allocation, the SCC and the knowledge accumulation distortions. Land allocation implies that region 1 which is an ID hot spot should increase its natural world relative to the noncooperative solution. Given that region 1 is expected to be the less developed region, this realization would support a policy of compensation from the developed region 2 to counterbalance losses in the production of the consumption composite. This compensation could be in the form of payments for ecosystem services, REDD+, or other policies which include transfer of resources from the developed to the developing world as for example is stated in the Paris Accord and subsequent Conferences of the Parties (COPs). The GHG distortion should be addressed by an appropriate increase in the SCC. Finally, correcting for the knowledge distortion could imply subsidizing knowledge accumulation in region 2 which would be reflected in the term $\frac{z_1 \hat{a}_1 a_{A,1} \beta_{L,A,1}}{N}$.

6.1.1 The socially optimal steady state

The knowledge system is decoupled from the climate system so the steady state can be characterized as in the noncooperative case. The steady state exists, it is unique with the saddle point property and indicates a higher level of knowledge at the steady state relative to the noncooperative steady state. This follows directly by comparing (64) with (83).

For the climate steady state the following proposition can be stated.

Proposition 4. *Assume that at the socially optimal solution,* $\left\{(\kappa_1^*(X), \kappa_2^*(X)), \left(\frac{\kappa_1^*(X)}{\partial X}, \frac{\kappa_2^*(X)}{\partial X}\right)\right\}$ *are positive, then a socially optimal steady state exists and has the saddle point property.*

For the proof, see Appendix.

Convergence to the steady state is shown in figure 7.

6.2 Model misspecification in the long-run social optimum and robust control

The impact of ambiguity in the short run was examined in section 4. In this section we study the impact of model misspecification which affects the evolution of the average temperature in each region which in turn affects the contact number. Since the impact of climate change on the emergence of IDs is an issue of current investigation, it is natural to associate misspecification concerns with this impact. This argument suggests that the regulator in each region is concerned about possible misspecification in the sense of Hansen et al. (2006) and Hansen and Sargent (2008) in the dynamics of the system.

We choose to introduce misspecification concerns in the dynamics of climate change. These concerns are introduced by allowing for a family of stochastic perturbations to a Brownian motion characterizing climate dynamics. The perturbations are defined in terms of measurable drift distortions. The misspecification error which expresses the decisions maker's concerns regarding departures from a benchmark model is reflected in an entropic constraint (Hansen et al. 2006; Hansen and Sargent 2008). Ambiguity and concerns about the possibility that "an adversarial agent" – often referred to as Nature – will choose not the benchmark model but another one within an entropy ball, which will harm the decision maker's objective, are reflected in a quadratic penalty term which is added to the regulator's objective. This type of ambiguity about the actual model versus the benchmark model has also been referred to as model uncertainty.

Hansen and Sargent call the decision maker's optimization problem with a quadratic penalty "the multiplier robust control problem". A crucial parameter of the problem is the robustness parameter, which reflects the decision maker's concerns about model uncertainty or his/her aversion to ambiguity. It has been shown that, as in the short-run model, as the robustness parameter which is positive tends to the limiting value of zero or infinity, the decision problem is reduced to the standard optimization problem under risk – that is, a problem with no ambiguity aversion. When the robustness parameter increases from zero, then concerns about model uncertainty increase.

These concerns can be introduced by allowing additive distortions to the GHG accumulation equation of the form

$$\sqrt{\epsilon}\sigma_0^T \left(\eta^T + z\right),$$

where σ_0 is volatility and ϵ is a small noise parameter, z is i.i.d and η represents distortions. These concerns will be translated into concerns about temperature anomalies through the TCRE multipliers and finally to concerns about the long-term part of contact number $\varphi_{0i}\left(R_1, T_1\right)$. If we consider a multiplier robust control problem (e.g., Hansen et al. 2006, Hansen and Sargent 2011), the penalty associated with the distortion relative to the benchmark model can be expressed as

$$\frac{\left(\eta^T\right)^2}{2\theta_i^T(\epsilon)}, \; j = R, T,$$

where $\theta_i^T(\epsilon)$ is the robustness parameter. It has been shown (Campi and James 1996) that if $\theta_i^T(\epsilon) = \theta_{i0}^T\epsilon$, then as $\epsilon \to 0$, the stochastic robust control problem is reduced to a simpler deterministic robust control problem. Assume that GHG evolution for a social planner or global regulator with misspecification concerns can be written as:

$$\dot{X} = E_1 + E_2 - dX + \sigma_0^T \eta(t). \tag{85}$$

Then the socially optimal management problem with concerns about model misspecification is:

$$J = \max_{\{u_i(t), R_i(t\}} \min_{\{\eta^T\}} \int_0^\infty \mathrm{e}^{-\rho t} \sum_{i=1,2} \left[\log C_i(t) + \psi_i \log R_i(t) + \frac{\theta_i^T \left(\eta^T\right)^2}{2} \right] dt,$$

subject to (85) and the rest of the constraints. Note that the social planner may have different regional robustness parameters. This could reflect the different impact in regional temperature and contact numbers when there are deviations from the benchmark model. The first-order condition for the choice of the distortion η by the fictitious adversarial (or minimizing) agent is:

$$\eta^T = \frac{-\lambda \sigma_0^T}{\theta_1^T + \theta_2^T}.$$

Then the evolution of the climate subsystem for (λ, X) under model misspecification concerns will be, after modifying (78) and (79),

$$\dot{\lambda} = (\rho + d)\,\lambda + \sum_{i=1,2} z_i \hat{a}_i \omega_i \Lambda_i X - \sum_{i=1,2} \kappa_i \frac{\partial \varphi_{0i}(R_1, \Lambda_1 X)}{\partial X}$$

$$\dot{X} = E_1^* + E_2^* - dX + \sigma_0^T \frac{-\lambda \sigma_0^T}{\theta_1^T + \theta_2^T}.$$

For $\theta_i^T < \infty$ and assuming that the conditions of Proposition 5 are satisfied, there will be convergence to the steady state along the stable manifold, which will be different than the path and the steady state without misspecification concerns. Let the new path be $X(t) + \delta^T(t)$; this would imply new paths for regional temperatures $\Lambda_i \left(X(t) + \delta^T(t) \right)$. Then the impact on the temperature-dependent contact number would be a new contact number $\varphi_{0i}^T \left(\bar{L}_1 - L_{A,1}, \Lambda_i \left(X(t) + \delta^T(t) \right) \right)$. If misspecification concerns lead to more conservative emissions policies, such policies would reduce the temperature-dependent contact number.

6.3 A global social optimization problem

We consider a global social optimization problem without time separation, which means that the regions are acting cooperatively at the containment stage as well as at the climate-land use policy stage, or that some World Authority implements policy. We seek to explore all the different externalities associated with the epi-econ model developed in this paper along with possible policy instruments. The generalized Hamiltonian associated with this optimization problem is:

$$\begin{aligned}\mathcal{H} = z_1 \left[\hat{a}_1 \ln C + \hat{b}_1 \ln \left(\bar{L}_1 - L_{A,1}\right)\right] + z_2 \left[\hat{a}_2 \ln C_2 + \hat{b}_2 \ln \left(\bar{L}_2 - L_{A,2}\right)\right] + \\ \lambda \left[E_1 (t) + E_2 (t) - dX\right] + \xi_2 \left[n_2 (t) - mN\right] + \\ \kappa_1 \left[\varphi_{01} \left(\bar{L}_1 - L_{A,1}, T_1\right) + \bar{\varphi}_{11} - l_{c,1} - l_{A,1}\right] + \\ \kappa_2 \left[\varphi_{02} \left(\bar{L}_1 - L_{A,1}, T_1\right) + \bar{\varphi}_{12} - l_{c,2} - l_{A,2}\right],\end{aligned} \tag{86}$$

where

$$\begin{aligned}\bar{\varphi}_{11} =& \varphi_{11} \left[b_1 v_1 - q_2(1 - S_2)\right] \\ \bar{\varphi}_{12} =& \varphi_{12} \left[b_2 v_2 - q_1(1 - S_1)\right]\end{aligned} \tag{87}$$

and (S_1, S_2) are defined as:

$$S_1 = \varphi_{11} \left[b_1 v_1 - q_2 \left(1 - S_2\right)\right] \tag{88}$$

$$S_2 = \varphi_{12} \left[b_2 v_2 - q_1 \left(1 - S_1\right)\right], \tag{89}$$

and the control vector includes the containment parameters, that is

$$\mathbf{u}_i (t) = \left(l_{c,i}(t), l_{A,i}(t), L_{A,i}(t), E_{c,i}(t), E_{A,i}(t), n_2(t), v_1(t), v_2(t)\right).$$

Then the socially optimal containment policy will be determined as

$$v_1^* = \frac{\kappa_1 \varphi_{11} b_1 + \kappa_2 q_1 \varphi_{11} b_1}{z_1 \hat{a}_1 c_{v_1}} \tag{90}$$

$$v_2^* = \frac{\kappa_2 \varphi_{12} b_2 + \kappa_1 q_2 \varphi_{12} b_2}{z_2 \hat{a}_2 c_{v_2}}. \tag{91}$$

The multipliers κ have the same interpretation as the multipliers ζ in section 3. The term $\kappa_2 q_1 \varphi_{11} b_1$ captures the extra benefits that containment policy in region 1 has on region 2, since reducing the infected in region 1 also generates benefits in region 2 because fewer infected are traveling to from 1 to 2 as can be seen from (89). The interpretation is the same for the term $\kappa_1 q_2 \varphi_{12} b_2$. The rest of the optimality conditions are the same as those corresponding to (73). The policy implications for the result indicated by (90),(91) is that the World Authority implementing the solution could subsidize for the extra cost associated with benefits $(\kappa_2 q_1 \varphi_{11} b_1, \kappa_1 q_2 \varphi_{12} b_2)$.

6.4 The full solution: linking the short run with the long run

In the analysis of the optimal short-term disease containment in section 3, R_1 and T_1 were treated as fixed exogenous parameters. The solution of the long-run problem implies that if the regions follow OLNE or social optimization policies, then the fixed R_1 and T_1 in the short run will be determined by the corresponding OLNE or socially optimal paths at each point in time. Thus the short-run optimal containment policy v_i^* will follow a path $v_i^*(t)$ which will be determined by the long-run solution at the time scale of the climate change and will eventually converge to the OLNE or the socially optimal steady state. Assuming that in the short run containment policies and susceptibles are determined by the Nash equilibrium, since each region follows own health policies, the solution can be interpreted as the fast time SIS system converging to the slow manifold of the climate system. The path of the Nash equilibrium will be the solution, for $i, j = 1, 2, i \neq j$, of the system

$$S_i(t) \quad = \varphi_{0i}\left(R_1(t), T_1(t)\right) + \varphi_{1i}\left[b_i\left(\frac{\varphi_{1i} b_i}{c_{v_i}}\right)\zeta_i(S_j(t)) - q_j\left(1 - S_j(t)\right)\right] \quad (92)$$

in which the paths for $R_1(t), T_1(t)$ are either the OLNE paths or the socially optimal paths. Thus the full solution can be thought of as pasting two types of solutions: (i) Long-run: OLNE in long-run control variables – Short-run: Nash equilibrium in short-run control variables; or (ii) Long-run: Social optimum in long-run control variables – Short-run: Nash equilibrium in short-run control variables. In the simulations section of the paper, we provide potential solution paths for these two solution concepts.

7 Numerical simulations

This paper builds a model that contains two interrelated – coupled – building blocks. The first embodies the ideas of epidemiologist, biologists and ecologists about IDs and their relationship with climate change and land use. The second is an economic model which includes a traditional economic optimization of an objective which incorporates controls which: (i) in the short run, optimally contain emerged IDs; and (ii) in the long run, by choosing optimal paths for GHG emissions, land use and R&D that supports the bioeconomy, control the emergence and the severity of IDs.

We point out that this section does not provide a calibration but rather a numerical simulation using what we consider as plausible values for the parameters which are shown in the Appendix (section 9.2). The main reason is that a full calibration would require, for example, parameter values such as Nature and climate-dependent contact numbers or efficiency of vaccination policies in different regions which are areas of current research in other scientific fields and whose estimation goes beyond the objectives of the current paper. Our simulations looked at from this point of view provide qualitative results which suggest that the theory developed in this paper is worth further study.

7.1 Nash equilibrium

Figure 2 depicts the Nash equilibrium discussed in section 3.1. For our parametrization, a Nash equilibrium exists and at the equilibrium solution the susceptibles act as strategic complements, so the containment effect in one region will help the other region.

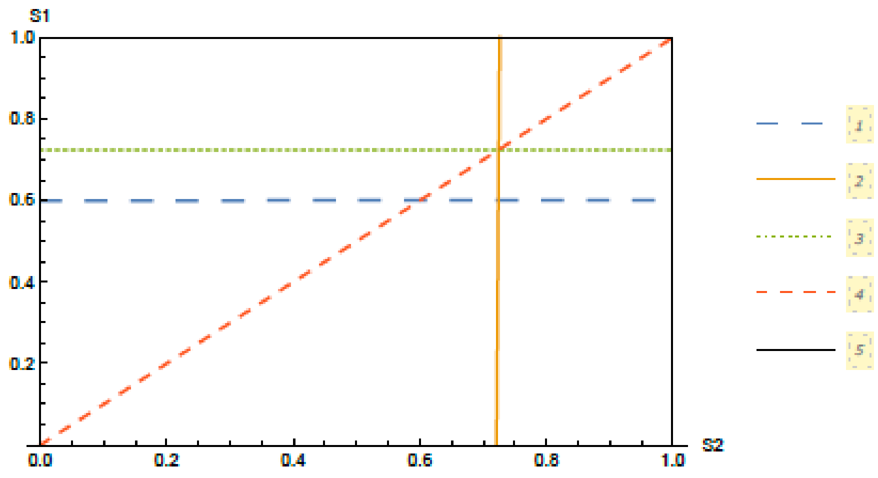

Figure 2: Nash equilibrium.

Nash equilibrium is at the intersection of lines 1 and 2 with $S_1 = 0.6, S_2 = 0.724$, which is the solution of the system of (29)-(30). Line 4 is the 45 degree line and its intersection with line 3 is the fixed point of (30), since $S_2^N : S_2^N = g_1 \left(g_2 (S_2^N) \right) = 0.724$, while line 5 with the vertical at $S_2 = 1$ defines the $[0, 1] \times [0, 1]$ space. The parametrization used implies contact numbers $(\sigma_1, \sigma_2) = (1.66, 1.28)$ at the Nash equilibrium solution. The definition of ζ_i in (27) and (24), labor allocation and energy use in the short run is a function of the equilibrium level of susceptibles $\left(S_1^N, S_2^N \right)$ and all constraints are satisfied. The Nash equilibrium value of susceptibles in region 2 relative to 1 is due to the parametrization in which it was assumed that the initial contact number was lower and the effectiveness of containment policy was higher in region 2 relative to region 1. Different parameterizations in the neighborhood of the benchmark one produced qualitatively similar results without any large shifts.

7.2 OLNE

To provide a tractable model we linearize that first-order conditions for OLNE around the Nash equilibrium and then we calibrate the constants of the emission functions (56), so that the steady state accumulation of CO_2 is approximately 3,300 $GtCO_2$ which is the IPCC (2021) prediction for the SSP1-6 scenario to be reached by around 2050. As mentioned earlier this exercised is not meant to provide "realistic" paths but to serve as a vehicle to clear up interrelated concepts and suggest that the model can provide an adequate description of a complex problem that combines epidemiology, climate science and economics. Figure 3 presents the OLNE steady state that makes clear the saddle point structure with a one-dimensional stable manifold in the three-dimensional state-costate space.

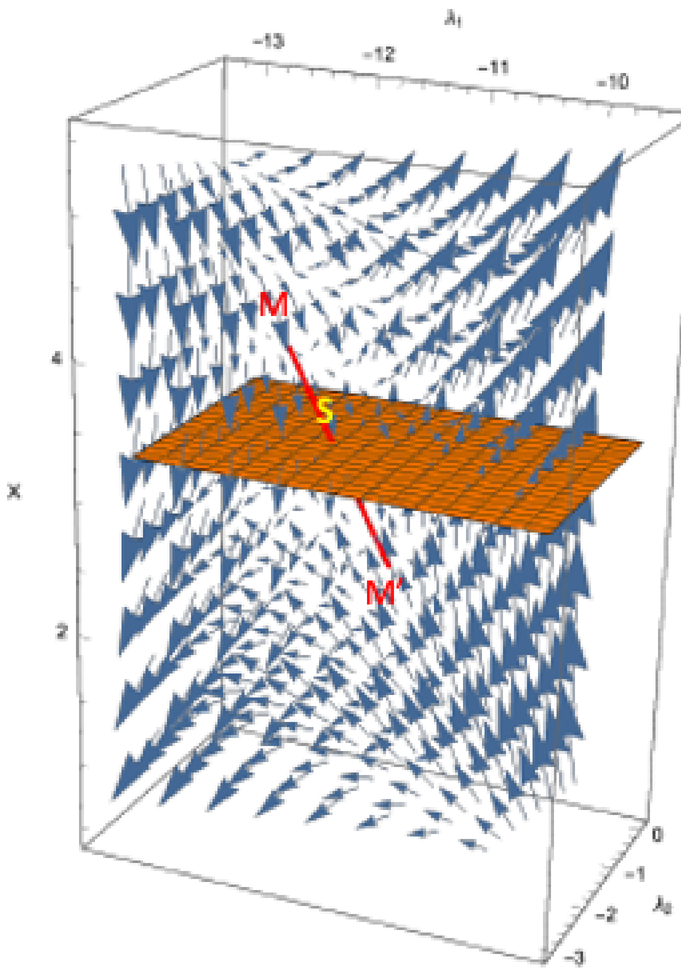

Figure 3: The OLNE in the three-dimensional state-costate space.

The stable manifold is MM' and in our parametrization the system's initial state is M'. This means that, given this initial state for the GHGs state variable X, initial values for the costates can be chosen by projecting M' on the (λ_1, λ_2) space such that the controlled system will converge along MM' to the OLNE steady state S. This steady state is $\lambda_1^* = -11.773, \lambda_2^* = -1.51234, X^* = 3.33054$. The costates have the usual interpretation of regional SCC and thus they take negative values as shadow costs. The SCC in region 1, the South, is higher than in the North because the South contains the ID reservoir and which could induce further costs as the temperature rises.[13]

Figure 4 presents the time paths for temperature and land use in region 1 along the stable manifold. The paths for region 2 have similar behavior but we present region 1 only because this is the relevant region for the ID.

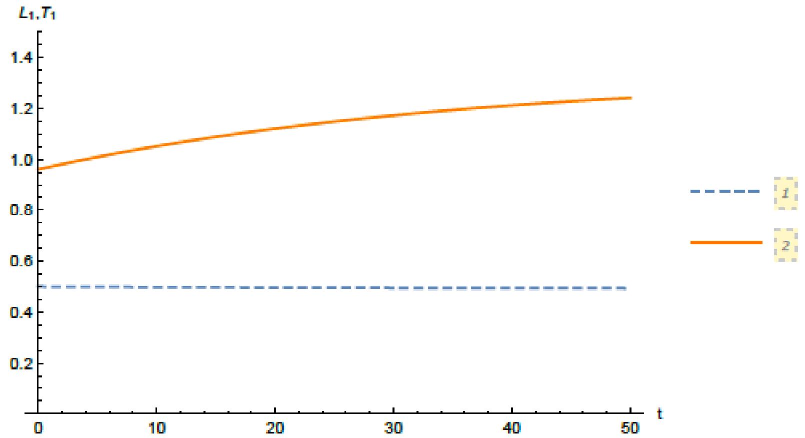

Figure 4: Time paths for temperature and land use in region 1 at the OLNE.

7.3 Knowledge accumulation, effective land use and the natural world

Using the parametrization of the Appendix (section 9.2), the knowledge steady state is $N^{\infty} = 1.285$ and it is shown in figure 5 along with the saddle point structure.

[13]All calculations and figures were produced using Mathematica 12. We are well aware that most of the "extra" digits in the numerical values are not significant, but we report them in the way the software reports numbers.

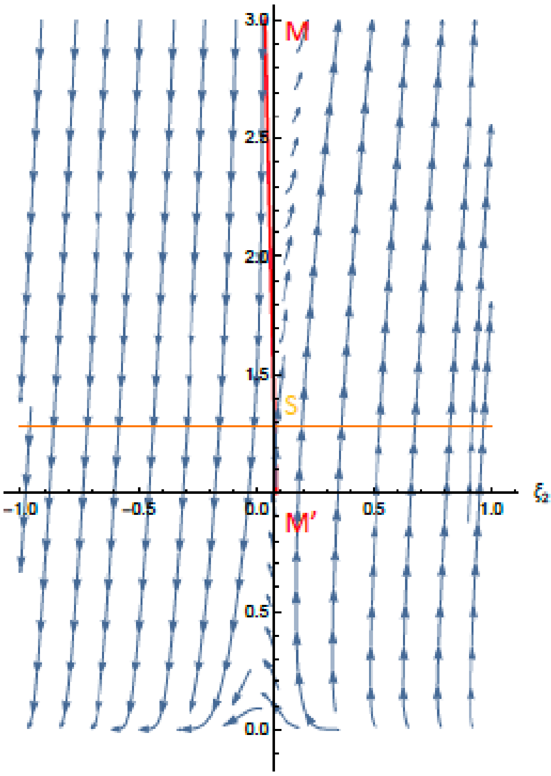

Figure 5: The saddle point steady state for knowledge.

The stable manifold is MM'. Starting from the initial state $N = 1$, at M', knowledge converges along the stable manifold to $N^{\infty} = 1.285$, following an optimal path $N^{*}(t)$. This implies that at the OLNE steady state the same agricultural output in the South can be produced with 22.2% less land relative to the case where no knowledge was generated in the North. This will reduce the severity of the epidemic in both the South and North. Since the original Hamiltonian system for knowledge is nonlinear, the linear manifold MM' should be regarded as the tangent to the nonlinear manifold at the steady state S.

From the OLNE equilibrium the optimal path for land use in agriculture in region 1 without R&D, (that is, $N = 1$ for all $t \geq 0$) is linear and declining in the temperature of region 1, since an increase in temperature is costly in terms of ID. Then, along the OLNE time path for temperature, the corresponding time path for land use is:

$$L_1^{*}(t) = 0.496899 + 0.00310047e^{-0.0878197t}. \tag{93}$$

If this path is combined with knowledge accumulation, then a new path for effective land is determined as $L_1^{EF}(t) = N^*(t)L_1^*(t)$. Assume that we want to keep effective land use equal to $L_1^*(t)$ so that the same effective land input is used but with less physical land, which will imply more land available for Nature. In this case a new path is defined as:

$$L_1^N(t) = \frac{L_1^*(t)}{N^*(t)} \text{ with } L_1^N(t) < L_1^*(t), t > 0.$$

The two paths $\left(L_1^N(t), L_1^*(t)\right)$ are shown in figure 6. The difference between the two paths corresponds to the increase in the natural world made possible due to knowledge accumulation.

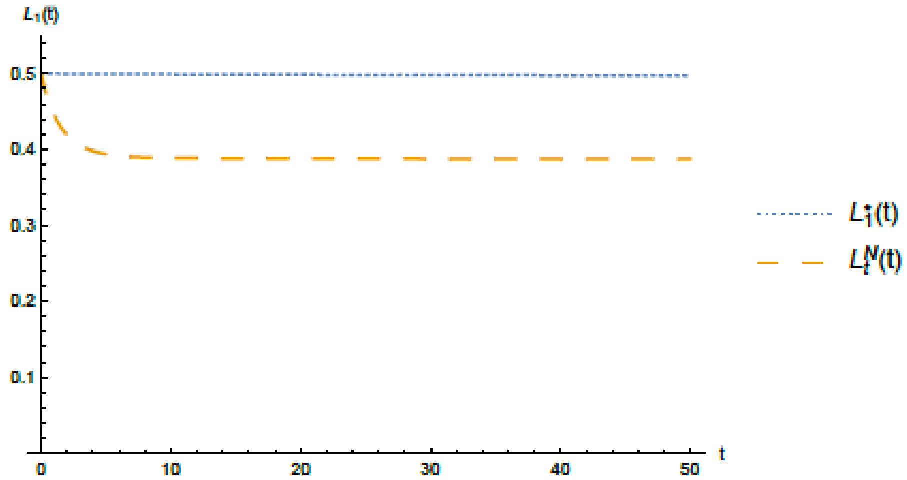

Figure 6: Gains in the natural world due to R&D.

The use of the $L_1^N(t)$ is expected to increase utility in both regions since it will reduce the ID cost without reducing land input.

7.4 The long-run social optimum

Using the linearization of the first order conditions and the same parametrization the socially optimal steady state with a clear the saddle point structure and an one-dimensional stable manifold in the two dimensional state-costates space is shown in figure 7.

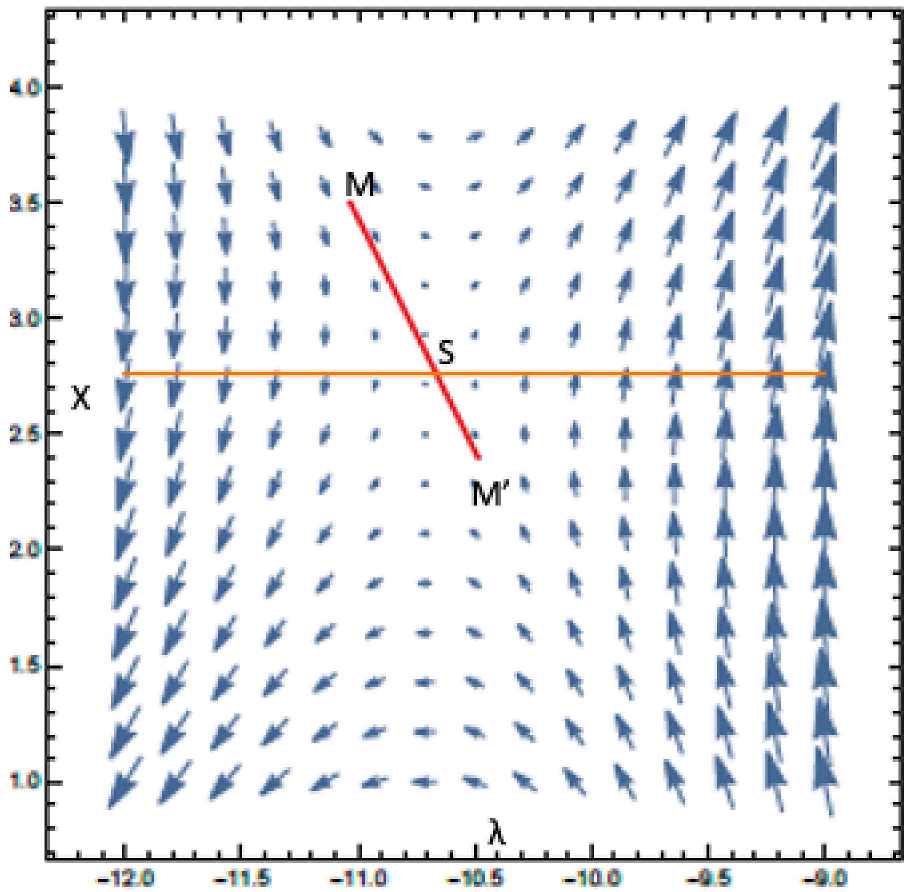

Figure 7: The socially optimal steady state.

The socially optimal steady state is $\lambda^*_{SO} = -10.669$, $X^*_{SO} = 2.76631$. The stable manifold starts from the initial state M' and converges to the steady state S. The SCC is lower for region 1 and higher for region 2 since all external costs have been internalized into the maximization of social welfare. The convergence to S indicates that at the social optimum the stock of GHG and regional temperatures are lower than at the OLNE steady state, as expected by theory. Figure 8 presents the time paths for temperature and land use in region 1 along the stable manifold.

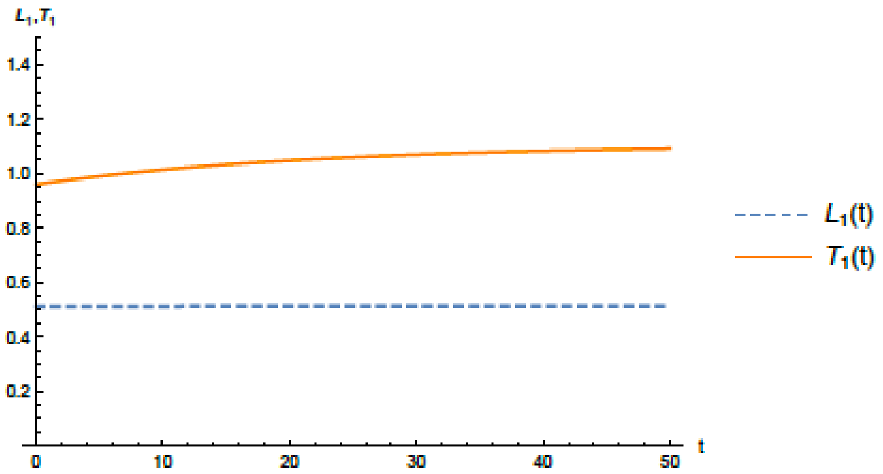

Figure 8: Time paths for temperature and land use in region 1 at the social optimum.

The temperature path is uniformly below the corresponding path under OLNE, shown in figure 4.

7.5 Linking the short run with the long run

We solve the system (92) for the short-run Nash equilibrium by using the values for $(L_1(t), T_1(t))$ corresponding to $t = \{0, 10, 20, 30, 40, 50, 60\}$ at the social optimum with land augmenting knowledge accumulation, and the OLNE with and without land augmenting knowledge accumulation, denoted in figures 9 and 10 as "SocOpt with R&D", "OLNE with R&D" and "OLNE" respectively. Land use with and without knowledge accumulation is shown in figure 6.

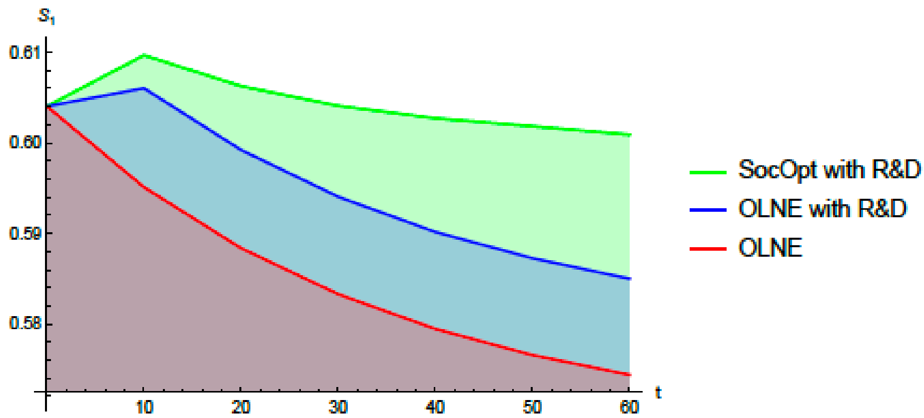

Figure 9: Susceptibles paths in region 1 with and without land augmenting knowledge accumulation.

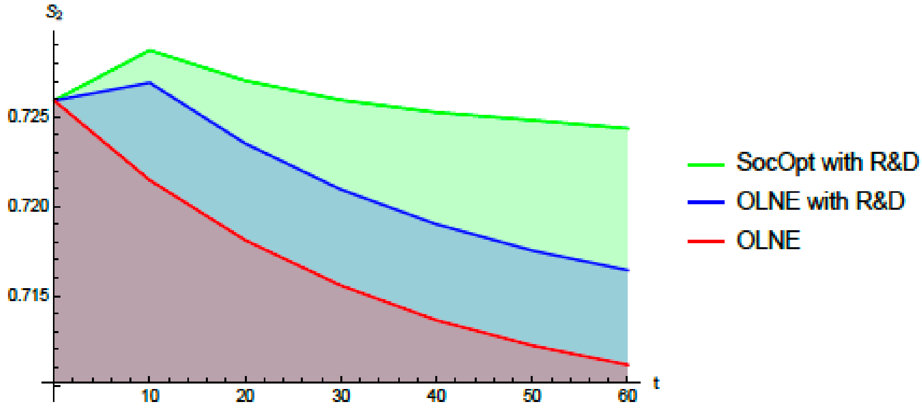

Figure 10: Susceptibles paths in region 2 with and without land augmenting knowledge accumulation.

The three lines represent the movement of the "fast" Nash equilibrium of the SIS subsystem along the "slow" stable manifold of the climate subsystem. The results suggest that land augmenting technical change helps to reduce the infectives, or increase the susceptibles, relative to the absence of such technical change, both at the OLNE and at the social optimum. As expected, at the social optimum susceptibles are higher relative to the OLNE. After the initial increase of the susceptibles because of the land-saving technical change, there is a continuous decrease because increasing temperatures increase the contact number, but susceptibles are always above the no technical change case. The difference between susceptibles with and without land augmenting knowledge accumulation shown in figures 9 and 10 persists until the climate subsystem reaches the steady-state OLNE or the socially optimal steady state, as shown in figures 3 and 7 respectively. Susceptibles in region 2 are higher relative to region 1 because of the particular parametrization as explained in section 7.1. Repeated runs with different parameterizations did not produce any change in the basic qualitative result. Land augmenting technical change increases the natural world and reduces the contact number of IDs. The result is stronger, the slower the increase in temperature.

8 Concluding remarks

We developed a two-region epi-econ model with the objective of studying short-term containment policy and long-term policies which focus on land-use changes and climate change as drivers of the emergence of IDs. We model noncooperation as short-run and long-run Nash equilibria. The short-run and long-run Nash equilibrium outcomes are compared with short- and long-run socially optimal policies for the world economy. The joint interaction of short run and long run in this type of fast-slow dynamic model is seldom studied, if at all, in the environmental management literature.

The insights emerging from this model suggest that noncooperative containment policies in the short run, during which land use and climate change effects are considered as fixed, generate – under plausible sufficient conditions – a Nash equilibrium outcome in the level of infections. Long-run noncooperative choices in land use policy are usefully modeled as an OLNE.

An important agenda for future research is to compare optimal welfare when controls and states at both time scales can be adjusted at the same time scale. Welfare comparison should also be studied under OLNE and feedback Nash equilibrium, when controls and states can be adjusted either at separate or at the same time scale. We have assumed the two time scales, fast and slow, are exogenously fixed. Both scales should be endogenous where the slow time scale can be speeded up with more resources devoted to that task. Some time scales of action are fixed by Nature, such as forest restoration. Furthermore, there are limits regarding how application of more costly effort can make trees of a given species, e.g., sequoias grow faster.

Ambiguity regarding the effectiveness of containment policies implies that increased concerns about the effectiveness of containment policies lead to weaker policies. The presence of strong ambiguity regarding the part of the containment number that depends on land use and climate change, and which is exogenous in the short run, could make necessary the introduction of additional policies, such as fines to supplement containment policies which are implemented on a voluntary basis.

The OLNE was characterized in the long run when the controls were land-use allocation between agriculture and the natural world, and carbon emissions in each region. In this equilibrium an additional positive externality, over and above existence values, emerges for the natural world while the SCC should be increased relative to the case when the emerging IDs are not taken into account. These adjustments result from the link between land use and climate change and the contact number of the emerging ID and should be taken into account in cost-benefit analysis. Ambiguity and concerns about model misspecification may lead to further increase in the SCC.

It was also shown that land augmenting technical change increases the land available to Nature and reduces the infectives relative to the case of no technical change. These results suggest that this type of technical change could be important in controlling infectious diseases, along with the other potential benefits in terms of augmented ecosystem services.

Further elaboration of the model could analyze productivity differences as well as differences in the quality of aggregate land endowments among regions and the associated impacts on regional policies, while a calibration of the model can be based on the parameters defined in Appendix 9.2.

In equations (8) and (9) which define the contact number as a function of policy parameters, the underlying assumption is that $X = \phi_{0i}\left(R_1(t), T_1(t)\right)$, and $Y = \phi_{1i}\left[b_i v\left(t\right)\right) - m_i^{as} S_i\left(t\right)) - q_j\left(1 - S_{jt}\right)]$ are perfect substitutes in "producing" non-infected people S. If, however, X, Y are producing S through a constant elasticity of substitution function with elasticity less than infinity, then there might be an upper bound in how much policies can increase S. Our conjecture is that this upper bound depends on Nature's undisturbed viral reserves and putting a bound on climate change. This could be an interesting area of further research. Introduction of accumulation of produced capital into the economic model and human capital for knowledge accumulation is another area of further research.

In summary, this paper makes a first attempt to create a formal quantitative multi-time scale framework where the policies against ID in the short run interact with long-run land use policies and human encroachment policies on areas of viral disease sources, as well as with human-induced climate change with uncertainties at both time scales. Detailed references are given to support the necessity of building this kind of "grand unified theory". We have only scratched the surface of this exciting, potentially important and unexplored research area.

9 Appendix

9.1 Proofs of Propositions

Proposition 1

The objective of the regulator in region $i = 1, 2$ for the noncooperative case becomes

$$J_i = \max_{u_i(t)} \left\{ \hat{a}_i \log C_i - \frac{1}{\theta} \ln \left(\mathbb{E} \exp \left[(-\theta) \zeta_i \varphi_{1i} b_i v_i \right] \right) \right\}, \tag{94}$$

and the first-order conditions for the optimal containment policy v_i imply

$$v_i^* = \frac{1}{c_{v_i}} \frac{\mathbb{E} \exp \left[(-\theta) \zeta_i(S_i) \varphi_{1i} b_i v_i \right] \zeta_i(S_i) \varphi_{1i} b_i}{\mathbb{E} \exp \left[(-\theta) \zeta_i(S_i) \varphi_{1i} b_i v_i \right]} = g\left(\theta, v_i; \zeta_i\right). \tag{95}$$

Assume that a Nash equilibrium for a given value of the robustness parameter θ exists. Taking the total derivative of both sides of the first-order conditions for the optimal containment policy v_i (95) with respect to v and θ, we obtain

$$\begin{aligned} c_i dv_i &= g_\theta d\theta + g_{v_{it}} dv_i \Rightarrow \left(c_i - g_{v_{it}}\right) \frac{dv_i}{d\theta} = g_\theta \text{ ,with} \\ g_\theta &= \frac{\partial \left[\frac{\mathbb{E} \exp\left[(-\theta)\zeta_i(S_i^N)\varphi_{1i} b_i v_i\right] \varphi_{1i} b_i}{\mathbb{E} \exp\left[(-\theta)\zeta_i(S_i^N)\varphi_{1i} b_i v_i\right]} \right]}{\partial \theta} = -\varphi_{1i} \zeta_i(S_i^N) v_i \hat{\sigma}_{b_i}^2 \\ g_{v_i} &= -\varphi_{1i} \theta \hat{\sigma}_{b_i}^2. \end{aligned}$$

Then it follows that

$$\frac{dv_i}{d\theta} = \frac{-\varphi_{1i} v_i \hat{\sigma}_{b_i}^2}{\left(c_i + \varphi_{1i} \zeta_i(S_i^N) \theta \hat{\sigma}_{b_i}^2\right)} < 0.$$

Proposition 2

Conditions (66), (67) imply the isoclines $N = \frac{\xi_2}{\hat{a}_2 c_{n_2} m}$, $N = \frac{\hat{a}_2 a_{H,2} \beta_{L,A,2}}{(\rho+m)\xi_2}$. The first is a ray from the origin with positive slope, while the second is a rectangular hyperbola in the positive quadrant. Both are continuous, therefore they intersect once at the steady state $\hat{(\xi_2^*, N^*)}$.

In system (63)-(65), let $\hat{A} = \frac{1}{\hat{a}_2 c_{n_2}}$, $\hat{B} = \hat{a}_2 \hat{a}_{A,2} \beta_{L,A,2}$. The linearized Jacobian for the system is

$$J=\begin{pmatrix} (\rho+m) & \frac{\hat{B}}{(N^{\infty})^2} \\ \frac{1}{\hat{A}} & -m \end{pmatrix}.$$

Since trace$J=\rho>0$ and det$J=-m(\rho+m)-\frac{1}{\hat{A}}\frac{\hat{B}}{N^{*2}}<0$, then the steady state $(\xi_2^{\infty},N^{\infty})$ has the saddle point property.

Proposition 3

The linearized system can be written as:

$$\dot{X}=\theta_0+\theta_1\lambda_1+\theta_2\lambda_2-dX \tag{96}$$

$$(\theta_0,\theta_1,\theta_2)>(0,0,0) \tag{97}$$

$$\dot{\lambda}_1=(\rho+d)\,\lambda_1+\omega_1\Lambda_1X+\kappa_1^*\gamma_{1T_1}\Lambda_1 \tag{98}$$

$$\kappa_1^*=\psi_{11}+\psi_{12}\Lambda_1X\ ,\ (\psi_{11},\psi_{12})>(0,0) \tag{99}$$

$$\dot{\lambda}_2=(\rho+d)\,\lambda_2+\omega_2\Lambda_2X+\kappa_2^*\gamma_{2T_1}\Lambda_1 \tag{100}$$

$$\kappa_2^*=\psi_{21}+\psi_{22}\Lambda_1X\ ,\ (\psi_{21},\psi_{22})>(0,0)\,. \tag{101}$$

The Hamiltonian system at the steady state can be written as

$$A\mathbf{x}=\mathbf{b} \tag{102}$$

$$A=\begin{pmatrix} (\rho+d) & 0 & J_{13}^C \\ 0 & (\rho+d) & J_{23}^C \\ \theta_1 & \theta_2 & -d \end{pmatrix},\mathbf{x}=\begin{pmatrix} \lambda_1 \\ \lambda_2 \\ X \end{pmatrix},\mathbf{b}=\begin{pmatrix} -\theta_0 \\ \psi_{11}\gamma_{1T_1}\Lambda_1 \\ \psi_{12}\gamma_{1T_1}\Lambda_1 \end{pmatrix}$$

$$J_{13}^C=(\omega_1\Lambda_1+\psi_{12}\Lambda_1^2\gamma_{1T_1})\,,\ J_{23}^C=(\omega_2\Lambda_2+\psi_{22}\Lambda_1^2\gamma_{2T_1}).$$

The eigenvalues of A are non-zero and real, two positive and one negative, or

$$\varrho_1=\rho+d$$

$$\varrho_{2,3}=\frac{1}{2}\left(\rho\pm\sqrt{4(\theta_1J_{13}^C+\theta_2J_{23}^C)+(\rho+2d)^2}\right).$$

The determinant of A is not zero because the product of eigenvalues of A is not zero, therefore the unique steady state can be obtained as a solution of the linear system (102), or

$$\mathbf{x}^{\infty} = A^{-1}\mathbf{b}.$$

Since there are one negative and two positive eigenvalues, the OLNE steady state has the saddle point property with a one-dimensional stable manifold.

Proposition 4

Using the linear version for the converse of the contact number and following the steps in the proof of Proposition 1, we solve (76) and (77) to obtain $(L_{A,1}, L_{A,2})$ as functions of (κ_1, κ_2). Substituting back in the relevant constraints along with the labor allocation condition we obtain $(\kappa_1^*(X), \kappa_2^*(X))$. The isoclines are then defined as:

$$|\lambda_{\dot{\lambda}=0} = \frac{-\sum_{i=1,2} z_i \hat{a}_i \omega_i \Lambda_i X - \sum_{i=1,2} \kappa_i^*(X) \gamma_{iT_1} \Lambda_1}{(\rho + d)} \quad (103)$$

$$|\lambda_{\dot{X}=0} = \frac{(\Gamma_1 + \Gamma_2) - (\chi_1 + \chi_2) X + \sqrt{-4\left[\chi_1\chi_2 - (\Gamma_1\chi_2 + \Gamma_1\chi_2)\right] + \left[(\chi_1 + \chi_2) X - (\Gamma_1 + \Gamma_2)\right]^2}}{2X} \quad (104)$$

where $\chi_i = z_i \hat{a}_i c_{E_i}$. If $\frac{\kappa_i^*(X)}{\partial X} > 0$, then (103) has the regular for these problems negative slope. If there is an interaction with a part of (104) that has a positive slope, then a steady state exists with the saddle point property. This can be shown by using the linearized, at this steady state, Jacobean matrix of the system (78),(79) which can be written as:

$$J^S = \begin{pmatrix} (\rho + d) & J_{12}^S \\ J_{21}^S & -d \end{pmatrix},$$

where $J_{12}^S = \left(\sum_{i=1,2} z_i \hat{a}_i \omega_i \Lambda_i + \sum_{i=1,2} \frac{\kappa_i^*(X)}{\partial X} \gamma_{iT_1} \Lambda_1\right) > 0$, $J_{21}^S = \frac{\partial\left(|\lambda_{\dot{X}=0}\right)}{\partial X} > 0$. Then trace$J^S > 0$, det$J^S < 0$ and the steady state has the saddle point property.

9.2 Model parameters

1. Consumption composite

$$Z_i(t) = C_i(t)^{\hat{a}_i} R_i(t)^{\hat{b}_i}, \hat{a}_i > 0, \hat{b}_i > 0, \hat{a}_i + \hat{b}_i < 1, i = 1, 2$$

$$C_i = \left[\left(l_{c,i}^{\beta_{l,c,i}} E_{c,i}^{\beta_{c,E,i}}\right)^{\alpha_{c,i}}\right] \times \left[\left(l_{A,i}^{\beta_{l,A,i}} \left(NL_{A,i}\right)^{\beta_{L,A,i}} E_{A,i}^{\beta_{E,A,i}}\right)^{\alpha_{A,i}}\right] \times$$
$$\exp\left[-\left(\sum_h w_{l,h,i} l_{h,i}\right) + \left(-c_{L,i} L_{A,i}\right) + \left(-\sum_h c_{E,h,i} E_{h,i}\right) + \right.$$
$$\left.\left(\frac{-c_{v,i} v_i^2}{2}\right) + \left(\frac{-\omega_i T_i^2}{2}\right) + \left(\frac{-c_{n,i} n_2^2}{2}\right)\right]$$

Parameter	Description	Value Region 1	Value Region 2
$\hat{a}_i$	Elasticities	0.7	0.8
$\hat{b}_i$	Elasticities	0.25	0.15
$\alpha_{c,i}$	Elasticities	0.7	0.9
$\beta_{l,c,i}$	Elasticities	0.95	0.8
$\beta_{c,E,i}$	Elasticities	0.05	0.2
$\alpha_{A,i}$	Elasticities	0.3	0.1
$\beta_{l,A,i}$	Elasticities	0.6	0.6
$\beta_{L,A,i}$	Elasticities	0.35	0.2
$\beta_{E,A,i}$	Elasticities	0.05	0.2
$c_{h,E,i}$	cost of energy $h = c, A$	$c_{cE} = 0.05, c_{cA} = 0.02$	$c_{cE} = c_{cA} = 0.025$
$w_{l,i}$	cost of labor use	0.3	0.78
$c_{L,i}$	cost of land use	0.1	0.2
c_{vi}	cost of containment	0.02	0.02
c_{ni}	cost of knowledge	-	0.45
m	knowledge depreciation	-	0.4
$\bar{L}$	regional natural world	1	1
$L_{A,1}$	natural world used*	0.5	0.5

(*) The values are fixed for short-run Nash.

2. The SIS model

$S_i(t)) \equiv \frac{1}{\sigma_i(t))} = \phi_{0i}(R(t), T(t)) + \phi_{1i}\left[b_i v(t)) - m_i^{as} S_i(t)) - q_j(1 - S_{jt})\right]$

Parameter	Description	Value Region 1	Value Region 2
ϕ_1	short-run impact on contact number	1	1
b	effectiveness of containment policy	0.1	0.6
m_i^{as}	infected asymptomatic	0.2	0.1
q	regional flow infected	$q_2 = 0.001$	$q_1 = 0.005$

R_0 fixed in the short run: 3.28 for COVID.

$\varphi_{0i}\left(R_1, T_1\right) = \gamma_{0i} + \gamma_{iR_i}\left(\bar{L}_1 - L_{A,1}\right) - \gamma_{iT_1} T_1$

Parameter	Description	Value Region 1	Value Region 2
γ_{0i}	exogenous component	0.65	0.75
γ_{iR_1}	natural world impact	0.1	0.05
γ_{iT_1}	climate change impact	0.1	0.05
θ_i	robustness parameter	free	free

The pre-containment σ are $\sigma_1 = 2.22, \sigma_2 = 1.48$ for temperature anomaly $T = 1$ the same for both regions.

3. Climate model

$\dot{X}(t) = E_1(t) + E_2(t) - dX(t)\ , X(0) = X_{preindustrial}$

$T_i = \Lambda_i X$

Parameter	Description	Value Region 1	Value Region 2
Λ_i	$T_i = \Lambda_i CE$	$\Lambda_1 = 0.4$	$\Lambda_2 = 0.54$
d	GHG depreciation[2]	0.00287	0.00287

With cumulative emissions CE2400GtCO_2 (IPCC 2021) and $T_1 = 0.96$ for the tropics and 1.031 for the Northern hemisphere (https://www.metoffce.gov.uk/hadobs/hadcrut4

4. Damage function: climate

$D_i(T_i) = \exp\left(\frac{-\omega_i T_i^2}{2}\right), T(0) = 0$ Preindustrial temperature anomaly

$T_i = \Lambda_i X$

Calibration for $3°C$ temperature anomaly, GDP loss in region 1 (Tropics-South) 15%, GDP loss in region 2 (North) 2% (Diffenbaugh and Burke 2019, Brock and Xepapadeas 2020).

Parameter	Description	Value Region 1	Value Region 2
$-\omega_i \Lambda_i^2$	damage coefficient	-0.0180577	-0.00338436

References

Almada AA, Golden CD, Osofsky SA, Myers SS (2017). A case for Planetary Health/GeoHealth. *GeoHealth*, 1, 75–78.

Augeraud-Véron E, Fabbri G, Schubert K (2020). Prevention and mitigation of epidemics: biodiversity conservation and confinement policies. Center for Economic Studies and Ifo Institute (CESifo), Working Paper No. 8506.

Barrows G, Sexton S, Zilberman D (2014). The impact of agricultural biotechnology on supply and land-use. *Environment and Development Economics*, 19(6), 676–703.

Berger L, Berger N, Bosetti V, Gilboa I, Hansen LP, Jarvis C, Marinacci M, Smith RD (2021). Rational policymaking during a pandemic. *PNAS*, 118, e2012704118.

Biswas N, Avinash Aslekar A (2022). Improving Agricultural Productivity: Use of Automation and Robotics. 2022 International Conference on Decision Aid Sciences and Applications (DASA).

Boppart T, Harmenberg K, Hassler J, Krusell P, Olsson J (2020). Confronting epidemics: the need for epi-econ IAMs. Konjunkturinstitutet. Available at https://www.konj.se/download/18.3891afad1764bc62ba84a0e3/1608119814917/Specials

Brock W, Xepapadeas A (2020). Regional climate policy under deep uncertainty: robust control and distributional concerns. *Environment and Development Economics*, https://doi.org/10. 1017/S1355770X20000248.

Campi MC, James RM (1996). Non-linear discrete time risk-sensitive optimal control. *International Journal of Robust and Nonlinear Control*, 6, 1–19.

Diffenbaugh N, Burke M (2019). Global warming has increased global economic inequality. *PNAS*, 116, 9808–9813.

Eichenbaum MS, Rebelo S, Trabandt M (2020). The macroeconomics of epidemics. National Bureau of Economic Research [preprint]. Available at http://doi.org/10.3386/ w26882.

ENSIA (2020). Destruction of habitat and loss of biodiversity are creating the perfect conditions for diseases like covid-19 to emerge. Available at https://ensia.com/features/covid-19-coronavirus-biodiversity-planetary-health-zoonoses/.

Evans T, Olson S, Watson J, Gruetzmacher K, Pruvot M, Jupiter S, Wang S, Clements T, Jung K (2020). Links between ecological integrity, emerging infectious diseases originating from wildlife, and other aspects of human health – an overview of the literature. The Wildlife Conservation Society. Available at https://oxfordinberlin.eu/files/wcslinksbetweenecologicalintegrityandeidsoriginatin

Foley JA, DeFries R, Asner GP, Barford C, Bonan G, Carpenter SR, Chapin FS, Coe MT, Daily GC, Gibbs HK, Helkowski JH (2005). Global consequences of land use. *Science*, 309(5734), 570–574.

Goodall J (2020). Jane Goodall: humanity is finished if it fails to adapt after Covid-19. *The Guardian*, 3 June 2020. Available at https://www.theguardian.com/science/2020 goodall-humanity-is-finished-if-it-fails-to-adapt-after-covid-19.

Hansen LP, Miao J (2018). Aversion to ambiguity and model misspecification in dynamic stochastic environments. *PNAS*, 115(37), 9163–9168.

Hansen LP, Sargent TJ (2008). *Robustness.* Princeton, NJ: Princeton University Press.

Hansen LP, Sargent TJ, Turmuhambetova G, Williams N (2006). Robust control and model misspecification. *Journal of Economic Theory*, 128(1), 45–90.

Hethcote HW (1989). Three basic epidemiological models. In Levin SA, Hallam TG, Gross LJ (eds), *Applied Mathematical Ecology.* Berlin, Heidelberg: Springer, pp. 119–144.

Hethcote HW (2000). The mathematics of infectious diseases. *SIAM Review*, 42(4), 599–653.

Institute of Medicine (2008). *Global Climate Change and Extreme Weather Events: Understanding the Contributions to Infectious Disease Emergence.* Workshop Summary. Washington, DC: The National Academies Press. Available at https://doi.org/10.17226/12435.

IPCC (2021). *Climate Change 2021: The Physical Science Basis. Contribution of Working Group I to the Sixth Assessment Report of the IPCC.* Cambridge University Press.

Lancet (2021). Enhancing Global Cooperation to End the COVID-19 Pandemic, The *LANCET* COVID-19 Commission. Available at https://covid19commission.org/enhan global-cooperation.

Leduc M, Matthews HD, de Elia R (2016). Regional estimates of the transient climate response to cumulative CO2 emissions. *Nature Climate Change*, 6, 474–478.

Marani M, Katul GG, Pan WK, Parolari AJ (2021). Intensity and frequency of extreme novel epidemics. *PNAS*, 118(35), e2105482118.

Matthews HD, Gillett NP, Stott PA, Zickfield K (2009). The proportionality of global warming to cumulative carbon emissions. *Nature*, 459, 829–833.

Meredith M, Sommerkorn M, Cassotta S, Derksen C, Ekaykin A, Hollowed A, Kofinas G, Mackintosh A, Melbourne-Thomas J, Muelbert MMC, Ottersen G, Hamish P, Schuur E (2019). Polar regions. In *IPCC Special Report on the Ocean and Cryosphere in a Changing Climate*, chapter 3.

Mora C, McKenzie T, Gaw IM, Dean JM, von Hammerstein H, Knudson TA, Setter RO, Smith CZ, Webster KM, Patz JA, Franklin EC (2022). Over half of known human pathogenic diseases can be aggravated by climate change. *Nature Climate Change*, 1–7.

Nova N, Athni TS, Childs ML, Mandle L, Mordecai EA (2022). Global change and emerging infectious diseases. *Annual Review of Resource Economics*, forthcoming.

Sachs J (2001). Tropical underdevelopment. NBER Working paper 8119, National Bureau of Economic Research.

Seierstad A, Sydsaeter K (1986). *Optimal Control Theory with Economic Applications*. Elsevier North-Holland, Inc.

Smith KF, Goldberg M, Rosenthal S, Carlson L, Chen J, Chen C, Ramachandran S (2014). Global rise in human infectious disease outbreaks. *Journal of the Royal Society Interface*, 11(101), http://dx.doi.org/10.1098/rsif.2014.0950.

The Independent Panel for Pandemic Preparedness and Response (2021). COVID-19: Make it the last pandemic. Available at https://www.unaids.org/en/resources/presscentr panel-pandemic-preparedness-response.

Thunström L, Newbold SC, Finnoff D, Ashworth M, Shogren JF (2020). The benefits and costs of using social distancing to flatten the curve for COVID-19. *Journal of Benefit-Cost Analysis*, 11(2), 179–195.

Walsh MG, De Smalen AW, Mor SM (2018). Climatic influence on anthrax suitability in warming northern latitudes. *Scientific Reports*, 8(1), doi:10.1038/s41598-018-27604-w.

Watts N, Amann M, Arnell N et al. (2021). The 2020 report of the *Lancet* Countdown on health and climate change: responding to converging crises. *Lancet*, 397, 129–170.

Wyns A (2020). Climate change and infectious diseases. *Scientific American*. Available at https://blogs.scientificamerican.com/observations/climate-change-and-infectious-diseases/.